Trabajo Fin de Máster
Ingeniería Química

Production of adsorbents derived from nut shells for H_2S removal

Autora: Angela Maiello
Tutor: Francisco Javier Gutiérrez Ortiz

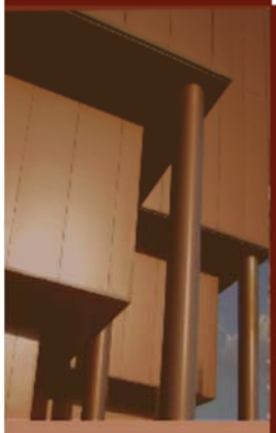

Dpto. Ingeniería Química y Ambiental
Escuela Técnica Superior de Ingeniería
Universidad de Sevilla

Sevilla, 2022

Trabajo Fin de Máster
Ingeniería Química

Production of adsorbents derived from nut shells for H_2S removal

Autora:
Angela Maiello

Tutor:
Francisco Javier Gutiérrez Ortiz
Catedrático de Universidad

Dpto. de Ingeniería Química y Ambiental
Escuela Técnica Superior de Ingeniería
Universidad de Sevilla
Sevilla, 2022

Trabajo Fin de Máster: Production of adsorbents derived from nut shells for H_2S removal

Autora: Angela Maiello
Tutor: Francisco Javier Gutiérrez Ortiz

El tribunal nombrado para juzgar el Proyecto arriba indicado, compuesto por los siguientes miembros:

Presidente:

Vocales:

Secretario:

Acuerdan otorgarle la calificación de:

Sevilla, 2022

El Secretario del Tribunal

INDEX

List of Tables

List of Figures

ABSTRACT

The goal of this study is to investigate the removal of H_2S from biogas, a sustainable gas made from the anaerobic digestion of organic waste, using adsorbents deriving from organic waste materials as precursors.

The elimination of H_2S is a critical step in biogas cleaning since this component can cause premature equipment deterioration, sulphur emissions as SO_2 upon combustion and requires a significant cost.

Due to the high cost of activated carbon, the key goal is to identify low-cost novel adsorbents for desulphurization. To this aim, different kind of nut shells were individuated among the wastes of the food industry, and walnuts and almond shells were selected for their large availability and specific properties as precursors of adsorbent materials. These two precursors were chosen because of the great production amounts available in both Italy and Spain; due to the high production, a substantial quantity of shells suitable for use as adsorbents may be obtained. In this study, both almonds and walnuts are produced in Spain, in particular originating in the municipality of El Arenal (Avila), located in the autonomous community of Castile and Leon.

The experimental study was carried out in the Department of Chemical and Environmental Engineering at the University of Seville (US).

To produce adsorbents, initially a jaw mill and a blade mill were used to grind the shells; then, an electromagnetic sieve was utilized to get the desired grain size; and finally, a tubular furnace was used for the activation steps, leading to the production of the final adsorbents.
A fixed bed column was employed for the adsorption experimental campaigns, having a height of 430 mm and a diameter of 30 mm. Experimental tests were carried out at room temperature and atmospheric pressure, aiming at testing the H_2S adsorption capacity of the produced adsorbents, while selecting the best performance for desulphurization of a model biogas.

CHAPTER 1. INTRODUCTION

1.1. Air Pollution

Air pollution is defined as "*any change in the normal composition or physical state of the atmospheric air, due to the presence in the air of one or more substances in such quantities and characteristics as to alter normal ambient and healthy air conditions; to compromise recreational activities and other legitimate uses of the environment; to alter biological resources and ecosystems, as well as public and private goods*," according to the EPA. As a result, air pollution occurs when any substances, such as gases, droplets, and particles, change the quality of the air. Consequentially, air pollution is a collection of adverse consequences that have an impact on the biosphere and, as a result, on humans.

It's important to distinguish between two sorts of pollution sources (*figure 1.1*):

- *Natural*, i.e., deriving from natural sources.
- *Anthropogenic*, i.e., caused by human activities.

The anthropogenic sources in turn are divided into:

- *Fixed*, which can be small or very centralized and of great potential.
- *Mobil*, e.g., related to transport.

Anthropogenic sources have a significant impact on environmental quality and are intimately tied to energy generation and consumption.

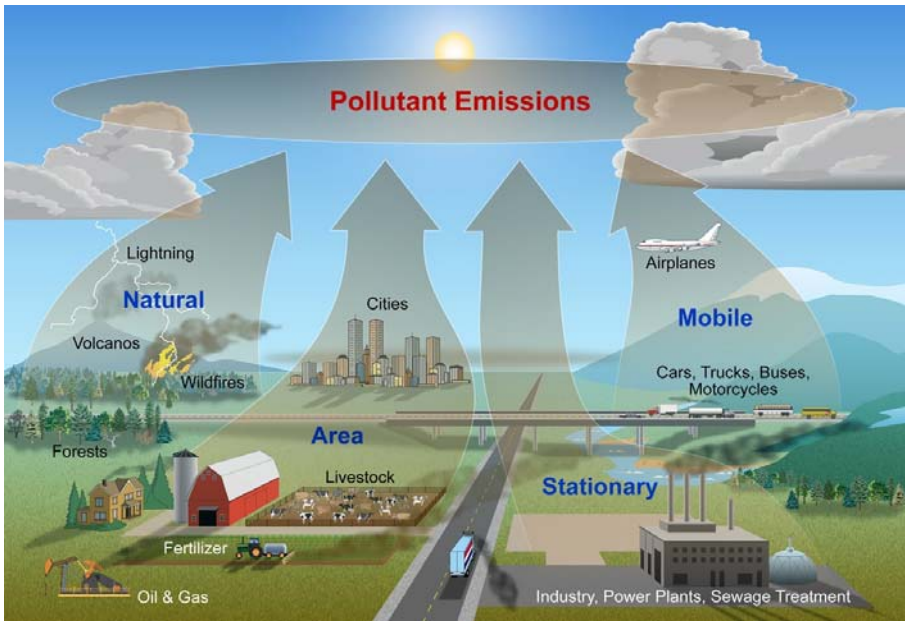

Figure 1. 1 - Pollutant emissions

Apart from that, pollutants released to the atmosphere can become reactive and generate new substances by solar light and the continuous recombination of reagents. As a result, the

course of such interactions should be investigated since they may result in the development of other compounds, which can be more or less dangerous to humans and the environment. In this sense, a distinction can be made between:

- *Primary pollutants*, which are harmful substances emitted directly to the atmosphere from the process that produced them, where they eventually undergo chemical-physical transformations.
- *Secondary pollutants*, which are produced by reactions between primary pollutants or between primary pollutants and natural atmospheric components. Secondary pollutants are a result of chemical-physical transformations, e.g., for the action of UV radiation or rain.

The pollutants are subject to diffusion, dispersion, and deposition phenomena after they are released to the atmosphere; additionally, they may undergo chemical-physical transformation processes that result in the production of new pollutants.

Approximately 3,000 air pollutants have been identified thus far, most of which are created by human activities such as industrial processes, transportation, or other anthropic processes. The pollutants' ways of formation and release are quite diverse, and there are numerous elements that can affect their diffusion in the atmosphere.

The main pollutants found in the atmosphere are certainly carbon monoxide (CO), carbon dioxide (CO_2), nitrogen compounds (NOx), particulates (PM) and among these we also find sulphur compounds (SOx).

1.1.1. Sulphur compounds

Sulphur is a common element that is vital to the environment's cycle. It's mostly found as sulphide and sulphate ores on land, and it's mostly found as dissolved sulphate in the oceans. Sulphur dioxide, elemental sulphur, sulfuric acid, hydrogen sulphide (together with other reduced sulphur species) and organic sulphur compounds are the most common sulphur compound found in the environment.

The existence of natural sulphur sources in the atmosphere has been recognised. We may surely locate geothermal activities among the different sources of sulphur compound emissions to the atmosphere; nonetheless, volcanoes produce by far the most of natural sulphur emissions; sulphur dioxide is the most common sulphur compound released. At low temperatures and under reducing conditions, hydrogen sulphide can compete, and lesser

quantities of sulphur trioxide, sulphate, and elemental sulphur are frequently present (Gordon G.E., 2000).

Fine spray, which forms above the oceans and consists of tiny droplets that evaporate to leave even smaller solid particles, is another key source of atmospheric sulphur.

The biological reduction of sulphur compounds is a significant natural source of sulphur in the atmosphere. This type of reduction occurs mainly in the presence of organic materials and in the absence of oxygen. Sulphur compounds are released to the atmosphere from non-specific sulphur reduction in marine algae, soils, and decaying plants, as well as by bacteria that selectively reduce certain sulphur compounds. Because of the quantitative nature of their reactions in the atmosphere, the quantities of volatile sulphur compounds produced by biogenic sources are nearly impossible to detect or compute directly (Cullis & Hirschler, 1980).

Sulphur compounds do not accumulate in the atmosphere, in fact, there is balance between the sulphur that we can find in the atmosphere and its return to the earth's surface, but man-made sulphate compounds released into the atmosphere can drastically change the balance point.

The overall sulphur released to the atmosphere by humans, as well as the influence of their activities, has been steadily rising over the years. The combustion of coal and petroleum, petroleum refining, and the smelting of non-ferrous ores are the main industrial sources of sulphur released to the atmosphere.

Coal and its by-products continue to be the most abundant source of sulphur in the atmosphere. Because of the high sulphur content of coal, this is one of the most significant sources of emissions. Sulphur emissions can be found in industrial and public utility combustion, as well as home and small-scale industry combustion.

Petroleum products are another significant producer of sulphur in the atmosphere. In previous years, the fraction of sulphur originated from petroleum had reached significant peaks. In this field, the principal sulphur compound produced and emitted to the atmosphere is sulphur dioxide.

Sulphur compounds are also released during the smelting of non-ferrous ore. Copper is the greatest contributor, with lead and zinc coming in second and third, respectively. This sort of pollution has been slowly decreasing over time (Cullis & Hirschler, 1980).

A significant sulphur content can be detected in many different types of fuel: natural gas (LPG/Biogas), Diesel, oils (ULSF, MGO/MDO, HFO (IFO)) and coal. Sulphur is found in minor amounts in natural gas compared to other fuels, and it is mostly in the form of H_2S.
In recent years, emissions from the use of sulphur-containing fuel have been greatly decreased, thanks to the use of fuel with much lower sulphur content than previously. Furthermore, thanks to the emission regulations enacted between 1990 and 2000, a significant reduction in various sorts of pollutants, particularly SO_x, has been detected (Clean Air Act). In an effort to protect the nation's air quality, the Clean Air Act (CAA) was first adopted in 1955 and then updated in 1990 and it's the foundational law that governs air quality in the United States of America. The purpose of the CAA is "to protect and enhance the quality of the Nation's air resources so as to promote the public health and welfare and the productive capacity of its population.". The Act establishes a broad and complicated regulatory framework for addressing fixed and mobile sources of air pollution. It requires the Environmental Protection Agency (EPA) to establish minimum national air quality standards and delegates primary enforcement and compliance duty to the different states. In addition, the Act establishes a permit system for all significant sources of pollution and addresses pollution prevention in areas where the air is clean.

Sulphur compounds are significant in the environment and climate system because they contribute to the generation of ozone depletion, the production of acid rain, and the corrosion of monuments and metals.

1.2. Biogas

Dangerous chemicals are discharged into the land, air, and water as a result of human activities, many of which are non-biodegradable and can cause lasting damage. The chemicals that anthropogenic activities release to the atmosphere alter the chemical composition of the air, causing sometimes irreversible damage to the environment and structures, as well as respiratory, dermatological, immunological, and liver disorders, as well as various types of cancer.
To reduce the amount of CO_2 and other pollutants released into the atmosphere, it is vital to reduce the use of fossil fuels and replace them with renewable energy sources. One of the most common renewable energy sources, whose production is constantly growing, is **biogas**.

Biogas typically refers to a gas produced by the biological breakdown of organic matter in the absence of oxygen. Biogas is a type of biofuel that is made from biogenic material, i.e., biodegradable elements such biomass, manure, sewage, urban waste, green waste, plant material, and energy crops that are digested or fermented anaerobically (Bhatia, 2014).

The main biodegradation process that leads to the formation of biogas is the anaerobic digestion of organic substances, performed by a consortium of microorganisms through a series of metabolic stages (hydrolysis, acidogenesis, acetogenesis and methanogenesis), in which different bacteria strains turn complex organic (liquid or solid) wastes into low molecular weight products (Dumont & Dumont, 2015). The uncontrolled degradation of wastes also leads to the formation of biogas that, is not opportunely contained, can give rise to significant emissions to atmosphere. Thus, the term "biogas" encompasses a wide range of gases resulting from various precursors, beginning with various organic wastes such as livestock manure, food waste, and sewage, which are all potential sources of biogenic gas, or biogas, which is usually considered a renewable energy source and is often classified according to the source (Speight, 2019).

From a composition point of view, biogas is a sustainable energy source that mostly consists of methane (CH_4) and carbon dioxide (CO_2). Various minor gases include nitrogen (N_2), water vapor (H_2O), ammonia (NH_3), hydrogen sulphide (H_2S), and other sulphur compounds. Biogas may also contain siloxanes, halogenated hydrocarbons, and volatile organic compounds (VOCs), depending on the producing site (landfills, wastewater treatment plants, plants handling industrial or food waste) (Dumont & Dumont, 2015).

Biogas has a high calorific power due to its high methane concentration, which is why it may be used as a renewable fuel. Biogas can also be utilized as a low-cost fuel, so this may be used to generate electricity, heat, and, like natural gas, can be compressed to be used as a biofuel for motor vehicles.

Biogas must be cleaned (mainly removing H_2O, H_2S and siloxane) and can be possibly upgraded (CO_2 removal) before it can be utilized as a source of energy (biomethane) to generate heat and power.

H_2S levels in biogas typically vary from 50 to 5,000 ppmv, but in certain situations can exceed 20,000 ppmv (2 vol%). The primary problems caused by high H_2S concentrations in biogas are (i) its corrosive activity, which can damage engines, pipelines, compressors, gas storage tanks, and (ii) the formation of sulphur oxides (SOx) as a result of H_2S combustion. Consequently, the content of H_2S in biogas must be decreased to values that do not harm combustion processes or cause SOx emissions (Speight, 2019).

In the **Table 1.1** a typical biogas composition is shown, evaluated considering different biogas production plants.

	Household waste	**Wastewater treatment plan sludge**	**Agricultural waste**
Methane CH_4 (% vol)	50 – 60	60 – 75	60 – 75
Carbon dioxide CO_2 (% vol)	30 – 40	20 – 35	20 – 35
Nitrogen N_2 (% vol)	0 – 5	0 - 1	0 – 1
Oxygen, O_2 (% vol)	0 – 1	< 0.5	< 0.5
Water, H_2O (% vol)	6 (~ 40°C)	6 (~ 40°C)	6 (~ 40°C)
Hydrogen sulphide, H_2S (mg/m^3)	100 – 900	1000 – 4000	3000 – 10.000
Ammonia, NH_3 (mg/m^3)	-	-	50 – 100

Table 1. 1 - Typical biogas composition (Speight, 2019)

1.3. Biogas pollutants: Hydrogen sulphide (H_2S)

Among the undesired substances commonly present in biogas, the compound of interest for the present work is hydrogen sulphide (H_2S).

Hydrogen sulphide is a colourless gas with the characteristic foul odour of rotten eggs, which is why it is called putrid gas. It has no acidic qualities in its anhydrous state, but it manifests in the presence of H_2O, when it forms aqueous sulphides and sulphydrates.

The olfactory perception of this chemical is noticeably low. It is a poisonous and highly combustible gas that can arise when exposed to air in specific quantities. It can have both natural origins, as it is present in the emissions of geothermal and volcanic zones and is produced by the bacterial degradation of animal and vegetable proteins, and anthropogenic origins.

Anthropic origin can be traced back to processes such as coking coal manufacturing, petroleum refining, fertilizer manufacture, wastewater treatment, and other industrial processes where it is an undesired by-product. Hydrogen sulphide is the principal by-product of petroleum hydro-desulfurization, and it can be found as an inherent component of natural petroleum or as a by-product of a substance's synthesis.

Hydrogen sulphide is exceedingly poisonous and unpleasant, as well as being asphyxiating. It paralyzes the olfactory nerve at high concentrations, making it impossible to detect its foul odour. The eyes and throat are irritated by low-level exposure. It can cause weariness, loss of appetite, headaches, memory problems, and disorientation in the long run. Concentrations higher than 1000 ppm cause instantaneous collapse by suffocation, even after a single breath, and the damage-free exposure limit for an 8-hour day is less than 10 ppm.

The gas is flammable, and at temperatures exceeding 260 °C, it burns with a bluish flame. H_2S concentrations in the air greater than 4% are explosive (WHO Regional Publication, 2000).

Figure 1.2 shows the structure of the hydrogen sulphide molecule and in the *figure 1.3* the 3D structure.

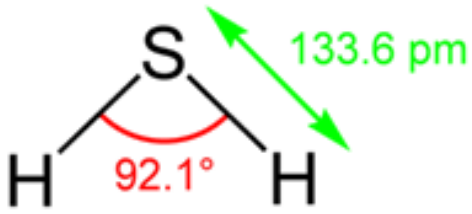

Figure 1. 2 - Hydrogen sulphide molecule structure

Figure 1. 3 - Hydrogen sulphide molecule 3D structure

Its chemical formula is H_2S, and the CAS number is 7783 06-4. The sulphur atom forms two polarized covalent bonds with two hydrogen atoms. The molecule is angled, with bond angle of 92.1°.

In the **Table 1.2** the properties of hydrogen sulphide are reported.

Because H_2S is rapidly oxidized by hydroxyl radicals and other atmospheric oxidants to SO_2 and then sulphate, the residence time of emitted H_2S in the atmosphere is short (about 15 days) (’Malone Rubright et al., 2017).

Properties	Value
Molecular Weight	34.08
Density (s.c.)	1.505 kg/m^3
Melting point	-82°C
Boiling point	-60°C
Solubility in water	4 g/dm^3 at 20°C
Vapor pressure	1740 kPa (at 21°C)
Acidity (pKa)	7.0
Thermal heat capacity	1.003 J/K*g
Standard molar entropy ($S°_{298}$ at 298K)	206 J/mol*K
Std enthalpy of formation ($\Delta_f H^{\ominus}298$)	-21 kJ/mol
Critical temperature	100.2 °C
Critical pressure	8.97 bar
Critical volume	0.00288 m^3/kg

Table 1. 2 - Properties of hydrogen sulphide

Figure 1.4 shows the participation of hydrogen sulphide in the overall sulphur cycle.

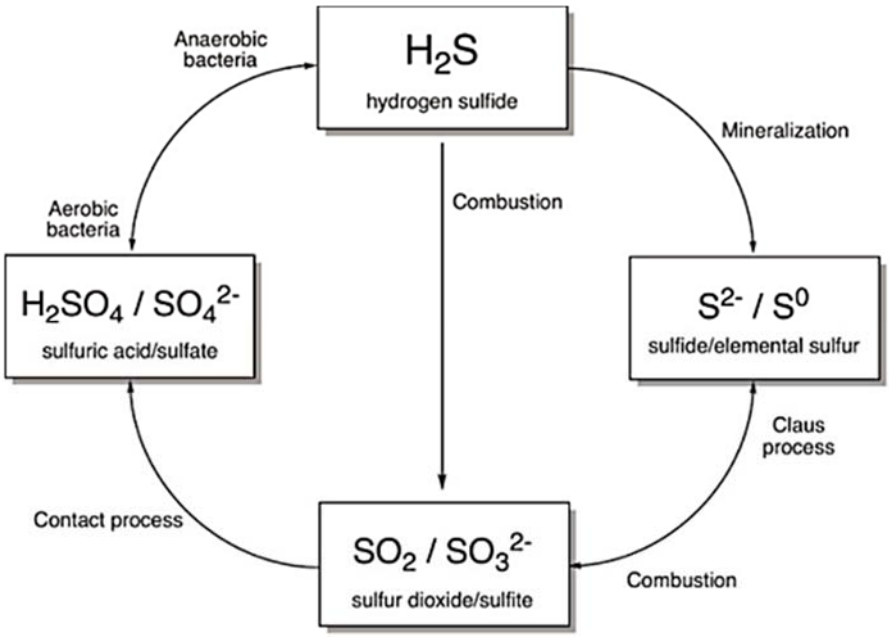

Figure 1. 4 - Sulphur cycle ('Malone Rubright et al., 2017)

As a result, H_2S concentrations in rural regions range from 0.02 to 0.3 ppb. H_2S concentrations may readily exceed the olfactory threshold level of 0.02 ppm in places with volcanic activity and contaminating industrial or animal output. Furthermore, air H_2S concentrations near volcanoes and geothermal wells may approach 0.1 ppm. Half of the population can detect the acrid odour of H_2S at quantities as low as 8 ppb, and 90% can detect its usual odour at 50 ppb.

The ways in which hydrogen sulphide enters the human body are three:

- by inhalation through the lungs.
- by oral route, especially by the digestion of contaminated substances absorbed in the intestinal tract, first of all water.
- through the skin.

Table 1.3 shows the main effects of H_2S against various concentrations in air as reported by the US Commission for the medical and biological effects of environmental pollutants (Rita D'orsogna & Chou, 2010).

Effects on humans	Value
Threshold for activation of smell	0.05 ppm
Offensive odour	3 ppm
Threshold for damage to vision	50 ppm
Olfactory paralysis	100 ppm
Pulmonary edema, acute intoxication	300 ppm
Nervous system damage, apnea	500 ppm
Collapse, paralysis, immediate death	1000 ppm

Table 1. 3 - Effect of H_2S on humans (Rita D'orsogna & Chou, 2010).

The toxic effects of H_2S are also present in animals and are similar to those for humans.

The effect of high H_2S levels on plants is perplexing. Although high ambient H_2S concentrations may have a deleterious impact on plant growth and survival, foliar H_2S uptake may play an important role in plant sulphur feeding.

1.4. Emissions regulation

The issue of emissions to the atmosphere is addressed at the European level in a variety of ways; in particular, the legislation on industrial emissions and the regulation on ambient air quality can be distinguished. Directive 2010/75/CE regulates emissions from industrial

establishments (the so-called Ied Directive, industrial emissions directive). The key references for ambient air quality standards are the following:

- *Directive 2004/107/CE* concerns arsenic, cadmium, mercury, nickel, and aromatic hydrocarbons in ambient air.
- *Directive 2008/50/CE*, which consolidated some existing directives on air quality and emission limits into a single legislative text.
- *Directive 2016/2284/UE*, which amends Directive 2003/35/CE and repeals Directive 2001/81/CE and deals with the reduction of national emissions of certain air pollutants.

Directive 2016/2282/UE, also called the NEC Directive, establishes new national commitments to reduce anthropogenic emissions of sulphur dioxide, nitrogen oxide, ammonia, volatile organic compounds and fine particulates. To this end, Member States of UE are required to adopt and implement national pollution control programmes; in addition, measures are planned to monitor pollutants and adverse impacts of air pollution on ecosystems as well as reporting requirements for collected data.

The aim is to achieve the long-term air quality objectives advocated by both the World Health Organisation (WHO – OMS) and the European Union in the areas of biodiversity, ecosystem protection, climate and energy (Rigo & Tronconi, 2020).

1.4.1. Emissions of H_2S

Limit values, alarm thresholds, and/or target air quality values for hydrogen sulphide are not defined under European legislation. In the absence of regulatory references, it is a common practice at the national and international levels to resort to the OMS-WHO guidance values (**Table 1.4**).

Concentration	Reference
150 μg/m^3 (average 24h)	WHO Guidelines ed. 2000
100 μg/m^3 > 1-14 days (average value over the period)	WHO – IPSC
20 μg/m^3 up to 90 days (average value over the period)	WHO – IPCS

Table 1. 4 - WHO guidance value for H_2S

1.5. H_2S removal techniques

As the removal of H_2S is necessary to avoid equipment damage and environmental poisoning problems related to the emission of sulphur compounds, various techniques have been

adopted for the removal of hydrogen sulphide from the biogas stream, such as physical/chemical absorption, precipitation of iron chloride, adsorption of metal oxide/hydroxide, membrane permeation, biological methods and adsorption on activated carbon; the latter is of particular interest to us.
Appropriate gas collection and abatement systems must be identified, planned, implemented, and appropriately managed in order to avoid the dangers associated with hydrogen sulphide exposure (Yang & Ge, 2016).

In general, H_2S removal methods can be divided into two categories based on their principles: traditional physical-chemical methods and biological methods. Biological solutions have advanced significantly in recent years, owing to their high removal efficiency (>99%) and cheaper operating costs as compared to physical-chemical procedures. Methods that combined physical-chemicals and biological technologies have been also developed (Allegue & Hinge, 2014).

H_2S removal can be done *in-situ*, i.e., directly in the digester, or after digestion, *ex-situ*.
The most commonly used in situ methods are:

- *Addition of salts/oxides of iron in the digester.*
- *Air/oxygen dosing in the digester.*

Iron chlorides, phosphates, or oxides can be directly added to the digester or a pre-storage tank's feed substrate. The most commonly used method is to add $FeCl_2$. Ferrous chloride ($FeCl_3$) and iron hydroxide ($Fe(OH)_3$ or $Fe(OH)_2$) in solid form can also be used. They then react with hydrogen sulphide to produce insoluble iron sulphide salts (FeS).
The precipitation reactions of the iron salt can be written as follows:

<u>*Ferrous chloride*</u>: $Fe^{+2} + S^{-2} \rightarrow FeS$ *(1. 1)*

<u>*Ferrous hydroxide*</u>: $2Fe(OH)_3 + H_2S \rightarrow 2Fe(OH)_2 + S + 2H_2O$ *(1. 2)*

$Fe(OH)_2 + H_2S \rightarrow FeS + 2H_2O$ *(1. 3)*

<u>*Ferric chloride:*</u> $2FeCl_3 + 3H_2S \rightarrow 2FeS + S + 6HCl$ *(1. 4)*

This approach is very efficient at lowering high H_2S levels, but it is less effective at achieving a low and stable H_2S level in the range of vehicle and gas grid injection demands. Averagely,

it allows reducing H_2S concentrations in biogas to a value between 200 and 100 ppm. A considerable excess of iron ions is required for removal to lower concentrations. This method can only be considered a partial removal process at this time, and it must be used in concert with another technology to achieve a 10 ppmv reduction (Allegue & Hinge, 2014).

The addition of air or oxygen straight into the digester or storage tank is another in-situ method. This technique is based on the biological aerobic oxidation of H_2S to elemental sulphur or sulphates conducted by *Thiobacillus* bacteria. The majority of those sulphide-oxidizing bacteria are autotrophic, hence they use inorganic carbon as carbon source (CO_2 from biogas). They do not require inoculation and grow on the surface of the digestate or on the digester's structure. The following reaction occurs in the biogas:

$$2H_2S + O_2 \rightarrow 2S + 2H_2O \qquad (1.5)$$

A little amount of O_2 (2-6%), needed for the reaction to take place, is introduced into the biogas, for example, by utilizing an air pump. H_2S reductions of 80-99 %, down to 20-200 ppm, can be achieved depending on temperature, response time, and the volume and location of the air. However, the remaining concentration may be too high for biogas to be used as a natural gas alternative (Ryckebosch et al., 2011).

Hydrogen sulphide removal techniques (*ex-situ*) are classified as follows:

- *Biological* (e.g., biofilters, bio scrubbers, activated sludge).
- *Physical - Chemical* (e.g., adsorption with activated carbon, absorption with water, chemical absorption, chemical scrubbers, membrane purification).

In biofilters, hydrogen sulphide is degraded biologically by microorganisms that colonize an organic medium and convert hydrogen sulphide to elemental sulphur and sulfuric acid, from which sulphates are formed. Because the microorganisms employed to remove H_2S are aerobic, they require oxygen. The traditional method of providing oxygen to a biofilter is to inject air (4-10%) directly into the gas stream. Bio-scrubbers and bio-tricking filters, which use an inorganic medium, are an alternative to biofilters. Biofilters and bio-trickling filters differ primarily in the type of the carrier material, which is organic in biofilters and inert in bio-trickling filters. As nutrients are not present in the bio-trickling filter material, they are provided to the microorganisms by recirculating a liquid phase through the reactor on a continuous basis. The bio-scrubbers are made up of two column reactors: in the first, the

material is absorbed into the counter-current liquid in a packed bed; in the second, where the liquid from the first reactor is discharged, the degradative processes are developed by specific bacteria. The absence of oxygen or nitrogen injection into the biogas stream is a benefit of this procedure in comparison to biofilters/bio-trickling filters. Higher specific operating costs are the associated disadvantages.

In physical absorption H_2S is removed by absorption in water or other solvents, such as methanol. Chemical absorption, on the other hand, occurs in washing towers or scrubbers, usually in a packed bed, where the gas to be treated comes into contact with the liquid absorbent solution in a counter-current flow, with the gas passing through the liquid phase. Different sorts of solutions can be used to remove hydrogen sulphide (for example, sodium hydroxide, hydrogen peroxide, etc...). The main downside of absorption is that it usually solves a problem with a contaminated gas stream by creating a contaminated liquid stream that needs to be treated further. Other drawbacks include a high initial investment cost as well as significant water and/or chemical use. High removal efficiency (up to 99%), a small footprint, and the capacity to manage a wide variety of pollution concentrations are all advantages.

Membrane separation involves using semipermeable membranes to separate H_2S from a gas stream by creating a partial pressure gradient across the membrane's semipermeable glassy or rubbery surface. The membrane is designed to allow passing gas or pollutant molecules through it preferentially, resulting in a more concentrated pollutant stream on one side. Two types of membrane systems exist: high pressure with gas phase on both sides, and low pressure with a liquid adsorbent on one side. Due to their high-cost membrane separation is not yet competitive for selective removal of H_2S (Allegue & Hinge, 2014).

Lastly, adsorption is the chemical-physical process by which a gas is captured on the surface of a solid material, such as activated carbon or crystalline material with high internal porosity (e.g., silica gel, zeolites). Once the pollutant has been captured and the solid is saturated, adsorption materials must be regenerated or discarded. In general, activated carbon adsorption is employed for low contaminant concentrations; for greater levels, impregnated carbon or catalytic carbon should be used. Adsorption is one of the most competitive

technologies for desulfurization, for its simplicity and efficiency (> 99%). Impregnated activated carbon and iron oxides are the most used products for removing H_2S from biogas.

In order to maximize removal efficiency, the aforementioned methods are frequently employed in conjunction with one another, depending on the quality and characteristics of the gas to be treated and the degree of hydrogen sulphide present (Panza, 2020).

1.6. Objective of the study

Adsorption was employed to remove H_2S from simulated biogas in this research. Adsorption is an efficient process for H_2S removal and activated carbon is commonly employed as an adsorbent.

Given the high cost of removing hydrogen sulphide from gaseous streams via adsorption using commercial activated carbon, there is a great attention and interest in developing new adsorbent from natural precursors, such as organic waste, to generate low-cost adsorbents. Walnut and almond shells, which were discovered to be waste items from the food sector, were used in this research. To this aim, different thermal treatments were tested for the activation of these precursors and to generate different adsorbents.

The major goal of this research is to assess the H_2S adsorption capacity of the produced adsorbents, simultaneously individuating the best performing among those synthesized.

This allows us to determine which of the adsorbents created can be employed as a substitute or supplement to commercial activated carbons for removing hydrogen sulphide from gaseous streams, particularly from biogas.

CHAPTER 2. ADSORPTION

Adsorption is the chosen technique to remove H_2S from simulated biogas streams, as mentioned in the previous chapter.

In this chapter, adsorption phenomena are presented, and the related process is described in all its aspects. Subsequently, a brief insight into adsorption on activated carbon is provided, by focusing the attention on the adsorbent produced starting from lignocellulosic precursors.

2.1. Key concepts of adsorption

Adsorption is a mass transfer phenomenon in which a molecule of a fluid phase chemical species (gas or liquid), called adsorbate, bonds to the surface of a solid, the adsorbent, with which it comes into contact, due to adhesive forces generated on the solid/fluid interface surface (*figure 2.1*).

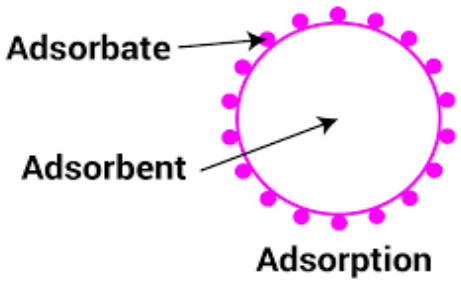

Figure 2. 1 - Representation of the adsorption

Thermodynamically, adsorption is an exothermic and spontaneous phenomenon, and this can be seen through the use of the Gibbs equation.

$$\Delta G = \Delta H - T\Delta S \qquad (2.\ 1)$$

In which ΔG is the Gibbs free energy variation, ΔH is the enthalpy variation, ΔS is the entropy variation, and T is the temperature.

Adsorption is a spontaneous process; hence it occurs with a decrease in the free energy of the system.

For spontaneous process, at constant pressure and temperature, we can write:

$$\Delta G = \Delta H - T\Delta S < 0 \qquad (2.\ 2)$$

As translational freedom of adsorbate is reduced when it is adsorbed, thus

$$\Delta S < 0 \qquad (2.3)$$

Because the process is spontaneous, ΔG is negative; consequently, ΔH must likewise be negative for the equation to be valid.; so, the process is exothermic and is therefore favoured at low temperatures.

$$\Delta H < 0 \qquad (2.4)$$

In terms of the bonds and forces of contact that are established between the adsorbent and the adsorbate, there are two types of adsorptions, i.e., physical and chemical adsorption.

In physical adsorption, adsorption is promoted by weak attractive forces (secondary bonds), such as Van der Waals forces, dipole-dipole bonds, hydrogen bonds. Physical adsorption is a non-selective process, that is, molecules can adsorb over the entire surface of the adsorbent.

In chemical adsorption, the bonds between adsorbed molecules and surface atoms are of chemical type. Chemical adsorption is specific, meaning that a solid surface can only chemisorb certain molecules at specified places on the surface, known as adsorption sites. Chemical adsorption is an active process, which means that it requires a particular activation energy. As a result, chemical adsorption is observed at greater temperatures than physical adsorption.

This means that the enthalpies involved in the two adsorptions are significantly different (higher for chemisorption); in fact, the heat of adsorption is frequently employed as a criterion for distinguishing the two processes.
Table 1.5 shows the main characteristics of chemical and physical adsorption.

In general, the adsorption process for a porous adsorbent material is characterized by a complex mechanism that can be schematized as follows:

- Transfer of pollutant matter from the bulk of the fluid to the surface of the adsorbent particle.
- Diffusion of the adsorbent within the pores of the adsorbent particle.
- Adsorption on the solid surface.

Thus, in addition to the chemical properties of the adsorbate and adsorbent, the fluid-dynamic properties of the gas stream play a crucial role in the entire process.

Physical Adsorption	Chemical Adsorption
Non-specific	Specific
Rapid, non-activated, reversible	Activated, may be slow and irreversible
Monolayer or Multilayer	Monolayer only
Only significant at relatively low temperatures	Possible over a wide range of temperatures
Enthalpies are in the region of -20 KJ/mol	Enthalpies are in the region of -200 KJ/mol
No electron transfer, although polarization of adsorbate may occur	Electron transfer leading to bond formation between adsorbate and adsorbent
As the temperature increases, process of physisorption decreases	With the increases in temperature, chemisorption first increases and then decreases

Table 2. 1 - Differences between physical and chemical adsorption

Because the adsorption phenomenon directly involves the adsorbent solid outer surface, the adsorption capacity is proportional to its specific surface; as a result, the most widely used industrial adsorbent materials are those with high porosity, such as activated carbon, silica gel, or appropriately treated natural materials.

2.2. Adsorption isotherms

The amount of gas adsorbed per gram of adsorbent is a function of temperature T, pressure P and the chemical nature of both the adsorbent and the adsorbate. The adsorbed quantity is a function of temperature and pressure once an adsorbent/adsorbed system has been defined. The temperature can then be set, and the amount of adsorbate as a function of pressure can be calculated.

The relationship between the adsorbed quantity per unit mass of sorbent and the partial pressure of the gas phase adsorbate (or its concentration, if in liquid phase) under equilibrium conditions at a fixed temperature is known as the *adsorption isotherm*. The realization of adsorption isotherms is used to conduct a thermodynamic analysis of adsorption phenomena.

The shape of the adsorption isotherm reveals the nature of the interactions taking place, the physic-chemical properties of the adsorbate and adsorbent, as well as the porosity characteristics.

Adsorbents' porosity properties can be classified according to pore characteristic size (IUPAC, 1972):

- *Macropores* are pores with a diameter higher than 50nm,
- *Mesopores* are pores with a diameter between 2 and 50nm
- *Micropores* are holes with a diameter less than 2nm.

2.2.1. IUPAC classification of isotherms

Isotherms are classified into six different types by IUPAC as part of physical adsorption. Brunauer S., Deming L. S., Deming W.S., and Teller E. developed the BDDT classification, which includes the first five categories of isotherms. The type VI isotherm is a newer and less common class of isotherm. *Figure 2.1* shows the classification of physisorption isotherms according to IUPAC (Sing, 1985).

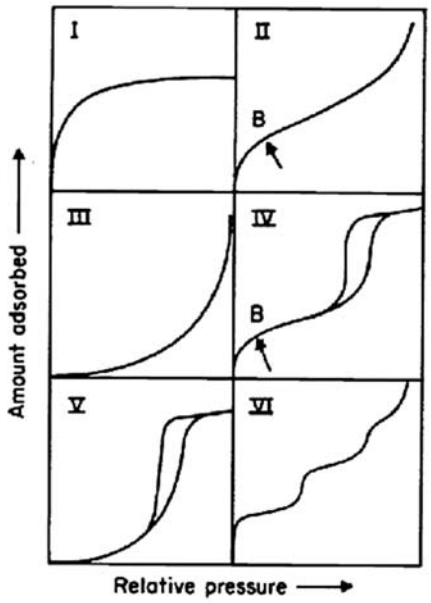

Figure 2. 2 - Types of physisorption isotherms

The relative pressure, which corresponds to the ratio between the partial pressure of the gas and the pressure at saturation of the gas at that temperature, is reported in the x-axis, while the amount adsorbed per unit mass is presented in the y-axis.

The Type I isotherm is concave in relation to x-axis (relative pressure), indicating that the adsorbed quantity does not grow continuously with pressure, but rather approaches to a limit value. The limit value is due to the presence of very small pores, which cannot be occupied by more than a single monomolecular layer. This kind is found in microporous materials having a small outer surface, such as active carbons, zeolites, and silica gel.

The Type II isotherm is generally observed in the adsorption of gases on macropores or non-porous solids. It shows a point of inflection that indicates the pressure at which the monolayer coverage is complete and multilayer adsorption about to begin. The pressure at which the monolayer is completed is indicated by the x-axis of the inflection point (point B in the *figure 2.2*), whereas the y-axis is the quantity of material required to cover the solid's surface with the first layer of molecules. The substance then continues adsorption, and the curve tends to diverge at relative pressure levels approaching one. In this scenario, as the relative pressure rises, the amount adsorbed rises as well, but the amount adsorbed does not tend to a limit value.

The Type III isotherm is convex in relation to relative pressure across the entire domain and does not show a point when monolayer molecular formation occurs. This sort of isotherm is uncommon, and it represents weak adsorbent-adsorbate bonds.

The Type IV isotherm is typical of mesoporous solids, such as alumina and silica. The hysteresis cycle is one of the properties of this curve, therefore the curve followed in the adsorption phase differs from the one followed in the desorption phase. Pore blockage and vapor condensation in mesoporous capillaries are the main responsible of this phenomenon. The phenomenon of capillary condensation causes liquid to form inside the pores even when the relative pressure is lower than the unit. The isotherm begins with the same profile as the Type II isotherm, in which monolayer formation occurs (point B) and is followed by multilayer formation.

The Type V isotherm is likewise unusual; it is linked to the Type III isotherm due to weak interactions between the solid and the adsorbate, and it has hysteresis associated with the pore filling and emptying mechanism. For instance, type V isotherms are observed for water adsorption on hydrophobic microporous and mesoporous adsorbents.

The Type VI isotherm represents layer-by-layer adsorption on a nonporous surface with a high degree of uniformity. The steps represent the filling stages of the individual layers, while the plateau sections indicate that nothing or very few gas is adsorbed for relative pressure ranges other than those at which the steps are observed. The step-height represents the capacity of each adsorbed layer, while the sharpness of the step is dependent on the system and temperature. Type VI isotherms obtained with argon or krypton at low temperatures on graphitised carbon blacks are among the best examples.

Because physisorption is a surface phenomenon, the fundamental parameters that govern the entire process are the specific surface exposed, or the area occupied by the pores, the total volume of pores, and the characteristic pore size, or the average pore diameter; thus, information on the porosity of the analysed material can be obtained from a qualitative analysis of an adsorption isotherm (Sing, 1985).

2.2.2. Adsorption models

The adsorption models that have been set up over time are all empirically grounded and allow for the interpretation of the phenomenon using parametric equations.

- **Isotherm of Langmuir**

The Langmuir model (1918) describes monolayer adsorption and is the most extensively used model in practical applications because it is straightforward to formulate mathematically and provides good feedback on the quality of the results.

This model was originally created for chemisorption, but it is equally applicable to physical adsorption on microporous solids since it takes into account the creation of a single molecular layer on the porous solid's surface.

The following are the hypotheses that underpin the Langmuir model:

1. The adsorption sites are energetically equivalent (homogeneous surface), which means that the adsorption heat is constant.
2. There are no lateral interactions between the molecules that have been adsorbed, then the adsorption heat is constant with the degree of coating.

These assumptions indicate that each site can only adsorb one adsorbate molecule and that each site's adsorption probability is the same.

To represent adsorption, the Langmuir model suggests the following dynamic scheme, indicating the equilibrium of the adsorption “pseudo-reaction”:

$$A_{(g)} + \sigma \rightleftarrows A\sigma \qquad (2.5)$$

Where A denotes the gas phase molecule, σ denotes the adsorption active sites, and Aσ denotes the adsorbed phase.

A kinetic constant, and thus a velocity, characterize both adsorption and desorption processes. At equilibrium, the velocity of the two processes equals, so we can derive the Langmuir isotherm equation:

$$w = \frac{w_{max} \cdot K \cdot P_{eq}}{1 + K \cdot P_{eq}} \qquad (2.6)$$

Where w is the amount of adsorbed solute (adsorption capacity), w_{max} is the maximum amount of adsorbable solute under conditions of monolayer formation, P_{eq} is the partial pressure of gas-phase adsorbate at equilibrium with solid phase and K is the thermodynamic equilibrium constant.

- **B.E.T. Theory**

The B.E.T. model, named from its formulators Brunauer, Emmett and Teller (1938), is an extension of the Langmuir model that is applicable to the notion of multilayer adsorption on a solid's surface.

This model is predicated on the following assumptions:

1. Equilibrium conditions are achieved by balancing the direct and reverse adsorption rates.
2. Active sites are assumed to be energetically equivalent, i.e., they have the same adsorption heat.
3. Lateral interactions between adsorbed molecules are assumed to be insignificant.
4. The possible formation of multilayer is considered: a distinction is made between an adsorptive heat q_1 relative to the first layer (solid-gas interaction) and an adsorption heat q_L relative to subsequent layers (interactions between layers of molecules), which is equivalent to the latent heat of condensation.

The B.E.T. equation is reported below, from which we may calculate the volume adsorbed in the monolayer:

$$\frac{P}{V(P^0 - P)} = \frac{C-1}{C\,V_m}\frac{P}{P^0} + \frac{1}{C \cdot V_m} \qquad (2.7)$$

In which P is the partial pressure of the gas, P^0 is the saturation pressure at that temperature, V is the volume adsorbed at a certain relative pressure, V_m is the volume of the monolayer and C is the constant of B.E.T., defined as:

$$C = e^{\frac{(q_1 - q_L)}{RT}} \qquad (2.\ 8)$$

The constants C and V_m are obtained by plotting $\frac{P}{V(P^0 - P)}$ as a function of $\frac{P}{P^0}$. The heat of adsorption in the first layer can thus be calculated using constant C.

- **Freundlich's Model**

Although the Langmuir model is one of the most often utilized in real systems, its hypotheses can be overly limiting in some circumstances; as a result, various expressions for the adsorption isotherm have been created over time. In reality, the idealized scenario of energy-equivalent adsorption sites is uncommon. It must be taken into account that there are repulsive forces between neighbouring adsorbed molecules on the surface of the adsorbent solid, as well as the presence of surface imperfections. These actions result in the formation of an adsorption heat field, which is dependent on the degree of surface coating.

The Freundlich isotherm is based on the idea that the solid surface is energetically heterogeneous, that the lower energy active sites are the most common, and that the energy distribution of the active sites declines exponentially. Monolayer adsorption is also assumed in this model. The expression of the Freundlich isotherm is as follows (van der Bruggen, 2014):

$$w = K \cdot P^{\frac{1}{n}} \qquad (2.\ 9)$$

In this equation, w in the adsorbed quantity, P is the partial pressure of the adsorbate in the gas, and *K* and *n* are empirical constants for each adsorbent-adsorbate pair at a given temperature.

2.3. Aspects of the adsorption kinetics

Fixed bed columns, packed with the adsorbent material and passed through the fluid stream holding the contaminating species to be removed, are the most extensively used plant configuration for adsorption operations. The adsorption kinetics tends to slow down as long as the gas stream decreases solute (pollutant) concentration by adsorption onto the fixed bed; thus, the driving force that regulates the mass transfer is reduced. As a result, the compositions of both the phases, fluid and solid, change both over time and along the position of the bed, as shown in *figure 2.3* (McCabe W.L. et al., 2005). For various time periods, the graph depicts typical adsorbed concentration profiles along the bed.

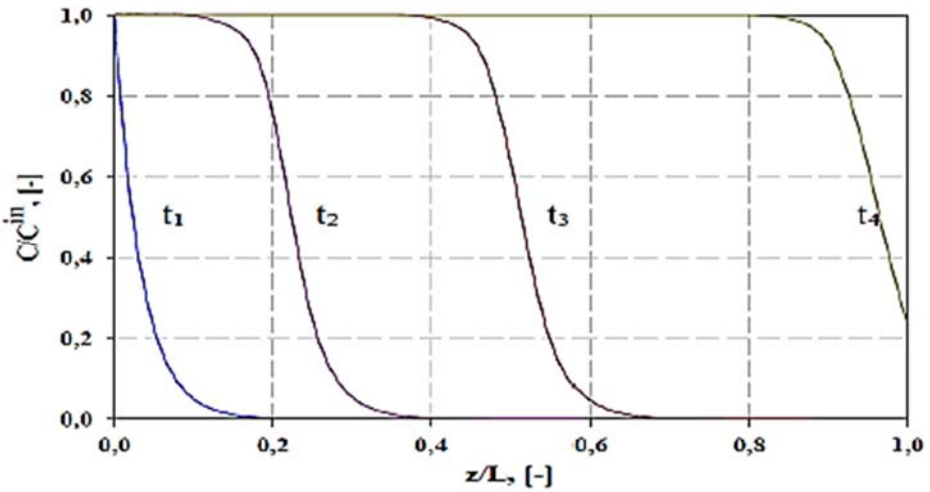

Figure 2. 3 - Concentration profiles for adsorption in fixed bed

The ratio between the adsorbate concentration in the fluid phase at a certain bed height and its concentration at column inlet is reported in the y-axis, whilst the dimensionless spatial coordinate is represented in the axis *z/L*, where L is the total length of the fixed bed.

The majority of mass transfer occurs near the bed inlet, where the fluid first gets in contact with the adsorbent. If the solid doesn't contain adsorbate, the concentration profile falls to zero exponentially before reaching the column's exit.

Curve t_1 in *figure 2.3* depicts this profile concentration. After certain time, the solid near the inlet is saturated, and the majority of mass transfer occurs further away from the inlet. As indicated by curve t_2, the concentration gradient becomes S-shaped.

The physical region where the greatest variation in adsorbate concentration occurs is the *Mass Transfer Zone* (MTZ), more precisely represents the area of the bed where a variation of C/C_0 occurs between 0.05 and 0.95. For times greater than t_1, the MTZ moves along the bed, since the layers that are always closer to the exit are saturated and the concentration profile assumes a sigmoidal pattern. At time t_4, the adsorbent is no longer able to capture all the pollutant discharged into the column and the output concentration is found to be different than zero.

The amplitude of MTZ is determined by the fluid dynamics and adsorption thermodynamics of the gas-solid system, then by the isotherm that regulates the adsorption process. The extension of MTZ area does not vary as the adsorption proceeds, but it moves along the bed towards its exit, until it is saturated.

The kinetic analysis of adsorption phenomena and the parameters that influence the performance is carried out using a process configuration that replicates, on a pilot scale, the real one, e.g., fixed-bed column, and by generating breakthrough curves. They are

experimental relations in which the pollutant concentration in the stream exiting the treatment column is related to time. The trend of a typical breakthrough curve is shown in *figure 2.4*.

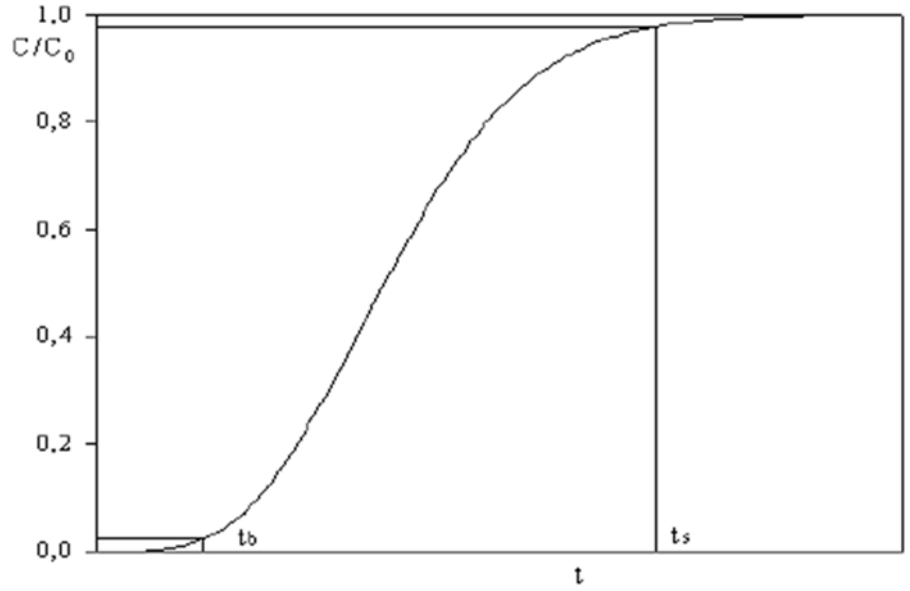

Figure 2. 4 - Characteristic trend of the breakthrough curve for adsorption in fixed bed

The profile has a sigmoidal trend, as shown in *figure 2.4*: at first, the pollutant is completely adsorbed by the solid, resulting in a zero-output concentration; as the initial layers of the column become saturated, the output concentration rises until the input level is reached, at which the solid is completely saturated. Two distinctive times, referred to as two levels of reference concentration (5% and 95% of C_0), characterize the breakthrough curve:

- the *breakpoint time*, t_b, denotes the time when $C/C_0=0.05$.
- the *saturation time*, t_s, denotes the time when $C/C_0=0.95$.

In general, the breakpoint time is set for the regulatory limit of permissible pollutant concentration in the effluent of the process from which it originates. As a result, this value represents the column's useful operating time, after which the current must be directed to a new adsorbent bed (McCabe W.L. et al., 2005).

From a material balance, it can be shown that the amount of matter adsorbed on the fully saturated bed is proportional to the area between the $C/C_0=1$ axis and the breakthrough curve, represented by the dotted area in *figure 2.5.*

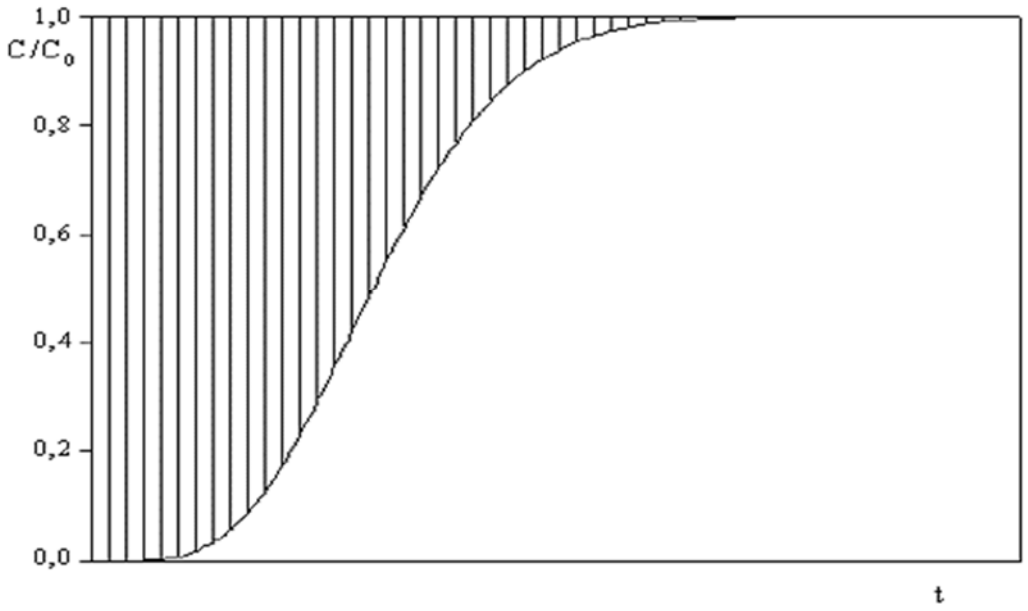

Figure 2. 5 - Evaluation of the maximum adsorbable amount

In fact, a differential material balance on the entire column can be performed to determine the sorbent's adsorption capacity.

$$Q^{IN}C_0dt - Q^{OUT}(t)C(t)dt = m \cdot w(t) \qquad (2.\ 10)$$

Where Q^{IN} and Q^{OUT} represent the volumetric flow rates of the gas stream in and out of the column, respectively; C_0 represents the concentration of the gas species at the inlet and C(t) represents the concentration of the gas species at the outlet; m is the mass of the adsorbent in column; w(t) represents the adsorption capacity of the solid, as a function of time.

By assuming a constant gas flow, it is possible to write:

$$\left(1 - \frac{C(t)}{C_0}\right)dt = \frac{m \cdot w(t)}{Q \cdot C_0} \qquad (2.\ 11)$$

Maximum adsorption capacity is achieved by integrating from zero to the instant when the bed is completely saturated, w_{sat}:

$$w_{sat} = \frac{QC_0 \cdot \int_0^{tsat}\left(1-\frac{C}{C_0}\right)dt}{m} \qquad (2.\ 12)$$

If we suppose to interrupt the column operation in correspondence of a fixed value of the C/C_0 ratio, e.g., the breakpoint, with C/C_0 equal to 0.05, the bed will be not entirely saturated. The near-saturated area of the adsorbent bed can be distinguished from the unused area, which is defined as the length of the unused bed (LUB). This value is calculated as the ratio of the adsorption capacity at saturation (w_{sat}), which is calculated over the whole

breakthrough curve, to the adsorption capacity w_{bp}, which is calculated up to the breakpoint value.

The adsorption capacity w_{bp} is defined as:

$$w_{bp} = \frac{QC_0 \cdot \int_0^{t_{bp}} \left(1 - \frac{C}{C_0}\right) dt}{m} \qquad (2.\ 13)$$

So, we can define LUB as:

$$LUB = \left(1 - \frac{w_{bp}}{w_{sat}}\right) L \qquad (2.\ 14)$$

Where L is the total length of the absorbent bed.

In addition, it is possible to derive the fraction of bed used, defined as the ratio between w_{bp} and w_{sat}:

$$F_{USB} = \frac{w_{bp}}{w_{sat}} = \frac{L - LUB}{L} = 1 - \frac{LBU}{L} \qquad (2.\ 15)$$

The LUB is independent of the length of the bed and is only affected by the fluid dynamics of the system and the adsorbing-adsorbent system. Indeed, increasing L, then the amount of solid, rigidly pushes the breakthrough curve along the time axis, but the region above for t > t_b remains unchanged.

It should be noted that this design parameter can only be evaluated if the isotherm is favourable (concavity downwards), as in this situation the MTZ's amplitude does not vary as it approaches the exit of the column.

From what stated, it is evident that the steeper the breakthrough curve appears, the more effective the system becomes, since it allows for better usage of the bed and hence a lower LUB.

2.4. Activated carbon

One of the most widely used adsorbent materials is activated carbon.

Activated carbon is a porous solid material made primarily of carbon atoms that is made from organic material (coal, wood, soot, synthetic polymers, etc.) through a carbonisation process, which involves heating in the absence of air at temperatures below 700 ° C. The substrate decomposes thermally at this point, and much of the non-carbonaceous material volatilizes, due to the pyrolysis process. Following that, employing a gaseous current at a temperature above 800 °C and an adequate thermal treatment of activation (gasification), all impurities are removed, resulting in an extension of the external surface and an increase in porosity. The activation process can also be conducted chemically, using surface treatments

with acids, bases, saline solutions or complexed agents, in order to give the coal its typical porous structure.

The activation causes the production of a huge number of pores that emerge across the entire mass of the carbon, giving it a large surface area ranging from 500 to 3000 m^2/g. The amount and measurement of pores present in an adsorbent are affected by the quality of the adsorbent, specifically the substance from which it is made, and the sort of activation process to which it is subjected.

From a chemical standpoint, activated carbon is made up of carbon atoms that are randomly distributed in planar graphite structures to form three-dimensional structures with a complex network of pores (*figure 2.6*). In comparison to the interior basal plane, the exterior carbonaceous structure has free surface valences, making the entire complex highly reactive.

Figure 2. 6 - Schematic representation of microstructure of activated carbon (Luka et al., 2018)

The activated carbons contain a variety of heteroatoms, the majority of which are oxygen, nitrogen, and certain inorganic elements, which are bonded together to create surface complexes that give the activated carbon its reactivity. The presence of oxygen, and hence the functional groups associated with it, is particularly important in the chemical behaviour of the solid.

The possible chemical structures that can be formed on the surface of activated carbon can be divided into six categories (Boehm, 2002):

- *Carboxylic functional groups.*
- *Lactonic functional groups.*
- *Phenolic functional groups.*
- *Carbonyl functional groups.*

- *Pyronic functional groups*
- *Heterocycles with carbon substitute oxygen atoms in the surface aromatic ring.*

The presence and properties of these groups appear to be a function of the activation process applied to raw coal. Low temperatures and the presence of oxygen, in particular, tend to give coal (L-carbons) an acidic character, whereas high temperatures and the lack of oxygen give it a basic character (H-carbons). The ability to adsorb specific compounds is determined by their presence; in some situations, it is possible to impregnate activated carbons with substances that improve their surface reactivity, which are selected according to the pollutant to be removed.

Activated carbons are employed for a variety of purposes in the treatment of fluid matrices, including the removal of organic and inorganic contaminants from liquid and gaseous streams, due to their adsorbent capabilities. They can be employed either in granular form (*Granular Activated Carbon – GAC*) or in powder form (*Powdered Activated Carbon – PAC*) for many applications (*figure 2.7*).

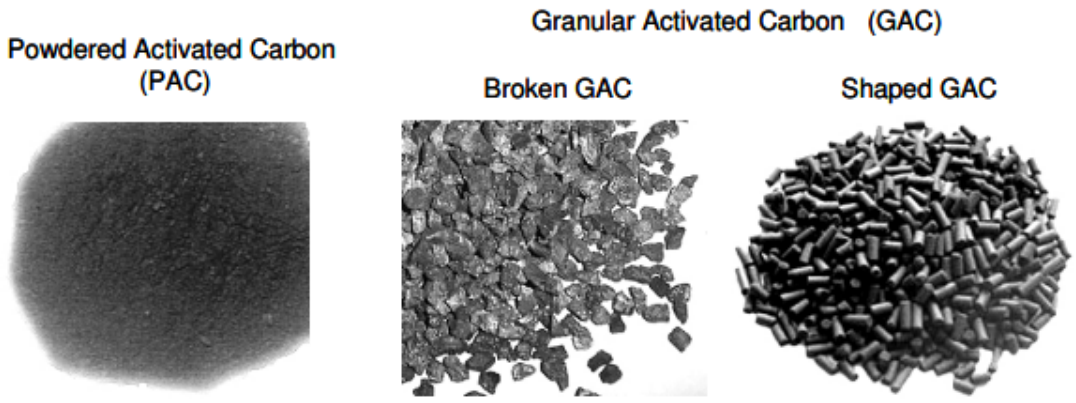

Figure 2. 7 - Types of activated carbons

Some compositional features of activated carbon can be used to assess its performance, including:

Bulk density: represents the weight of dry carbon per unit volume of carbon, including the volume of pores and voids between grains. Its value is determined by porosity and is hence linked to the activation process.

Particle density: is the weight for unit volume, including volume of the pores.

Humidity: is the percentage by weight of water adsorbed by activated carbon under standard conditions (P= 1 atm; T=20°C).

Ash content: is a purity index and represents the weight percentage of inorganic materials, such as aluminium oxides, silicon and iron, calcium salts. The quality of the carbon is better if the ash content is low.

Particle size distribution: characterizes the grain size of carbon and provides an indication on the uniformity of its size.

Surface B.E.T.: represents the specific surface area actually available for adsorption, evaluated through the surface available for adsorption of a nitrogen monolayer, whose molecule is small enough to have access to micropores.

Total pore volume: is the specific volume of the internal voids of a carbon particle, evaluated through the input of nitrogen or mercury gas.

2.5. Adsorbents used for H_2S removal

The choice of a suitable material for the removal of H_2S is a fundamental step for the adsorption process, as the material must comply with important requirements.

Many investigations have been conducted in order to create practical and high-performance solid sorbent materials with high sulphur capacity and selectivity, thermal durability, and good reproducibility for use in H_2S adsorptive removal processes, especially at low temperatures. The most acceptable materials utilized as an adsorbent or support for H_2S removal from various gas streams are porous materials with high surface area and large pore volume. Under various working conditions, zeolites, mesoporous silicas, porous carbon materials, activated carbons, and porous metal oxides are the most adopted materials because of their exceptional desulfurization capability. Apart from these traditional porous adsorbents, porous metal-organic frameworks (MOFs) have recently received much interest due to their high adsorption capabilities and ease of tenability in the effective adsorptive removal of H_2S (Khabazipour & Anbia, 2019).

The most adopted adsorbents for H_2S removal are described below with their key properties (*figure 2.8*).

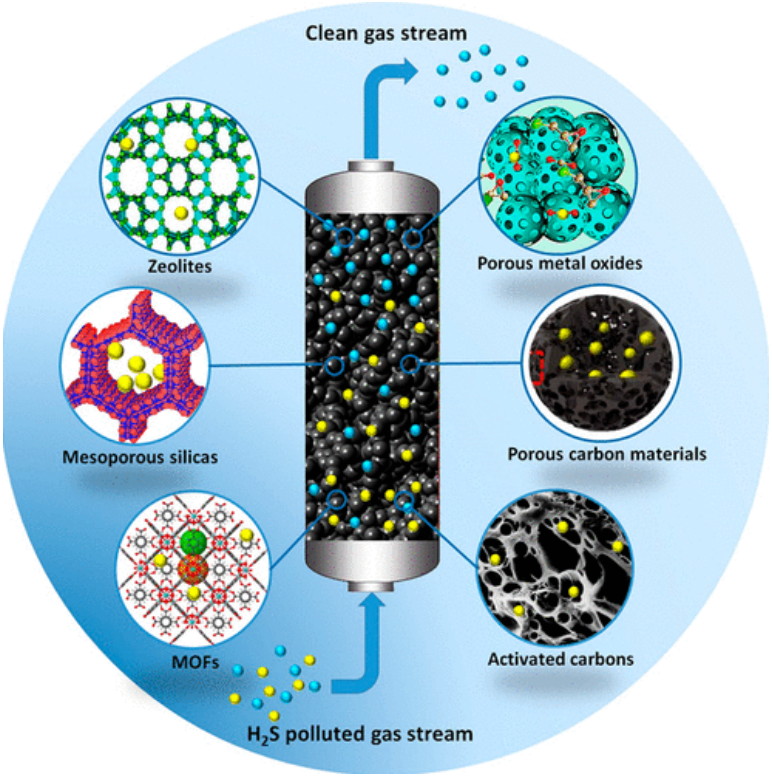

Figure 2. 8 - Types of adsorbents for H_2S removal

2.5.1. Porous metal oxides

Since 1970, several metal oxides, particularly metal oxide adsorbents of Zu, Cu, Fe, Mn, Co, Mo, and Ca, have been discovered to have the capacity to desulphurize high-temperature gases. The removal of hydrogen sulphide by metal oxides may entail physisorption onto the surface of a solid sorbent, followed by reactivity with the active phase to make sulphides, or a redox reaction with surface oxygen species to produce sulphates or elemental sulphur. Because of their large particle size, low surface areas, poor dispersion, and insufficient porosity, bulk metal oxides have a low sulfidation rate. Desulfurization performance could be improved by synthesizing novel materials with open macro and mesopores. Additional H_2S adsorption sites and improved diffusion through the internal open pores are provided by porous metal oxides with large surface areas and high porosity.

The ability of nanocrystalline mesoporous iron oxide (Fe_2O_3) to remove H_2S was examined, and it was discovered that the H_2S adsorption capacity was highly dependent on the pore volume and hydroxyl groups of the sorbent. In comparison to iron oxide, mesoporous Fe_2O_3 has a larger surface area, a greater number of mesopores, and a smaller crystal size, resulting in higher sulphur capacities.

Because they would quickly sinter and aggregate throughout the cycle of sulfidation/regeneration operations at high temperatures, the use of unsupported metal oxides could reduce desulfurization performance. Dispersing metal oxides onto supports with a large surface area and porous structure is an ideal technique to overcome the above constraint. The materials utilized to support the process should be inert, have a wide surface area, big pore size and volume, and strong mechanical and thermal stability. Various porous materials have been employed as supports to load various metal oxides; for example, efficient sorbents were created by loading 20%wt Fe_2O_3 on a porous alumina (Al_2O_3) substrate. Also tested was an adsorbent made of a mixed Zn and Cu active phase supported on mesoporous γ-alumina.

Recently, studies have been focused on low working temperatures for the removal of H_2S by metal oxides. Low temperatures (under 400°C) are preferable to high-temperature desulfurization because they are less expensive to operate. Furthermore, high temperatures can cause metal oxides to sinter, lowering their activity. At low working temperatures, however, sulfidation kinetics are considerably slowed, resulting in a decrease in the H_2S adsorption reaction with metal oxides and higher diffusion resistance. In the temperature range of 25-250°C, mesoporous cobalt oxides had a very high H_2S adsorption capability. The sulphur capacities of mesoporous Cr_2O_3, Mn_2O_3, CuO, and Fe_2O_3 were also shown to be higher than nonporous analogues, owing to their mesostructured (Khabazipour & Anbia, 2019).

2.5.2. Porous carbon materials

Due to intriguing properties such as large surface area and high micropores volume, several researchers have explored the efficacy of porous carbon materials (PCMs) for H_2S removal, e.g., mesoporous carbon aerogels and mesoporous carbon spheres. Despite the huge number of pores on the PCMs structure, the microporous structure can limit the analyte access to adsorption sites. The introduction of bigger pores into the PCM structure, such as mesopores and macropores, could improve adsorption effectiveness by providing more pathways for intrapore mass transfer. In addition to porosity, the surface chemistry of PMCs is an important parameter when dealing with polar contaminants like H_2S. PCMs have a poor adsorption behaviour toward acidic gases such as H_2S due to their hydrophobic nature. As a result, substantial studies have been devoted to overcoming this difficulty and enhance their

H_2S removal effectiveness through structural modifications such as alkaline chemical impregnation and heteroatom doping (Khabazipour & Anbia, 2019).

2.5.3. Activated carbon

Activated carbon (AC) is widely utilized as a superior adsorbent in separation processes because to its large specific surface area, high pore volume, and ability to be modified. Furthermore, when compared to other adsorbents such as zeolites, alumina, and silica, this material is comparatively inexpensive. Activated carbon can be made from a variety of carbon sources, including wood, coconut shell, and so on, with varying porosity, fixed carbon content, and ash, depending on the initial source and carbonizing procedure.

Activated carbon can remove H_2S through a variety of ways. Activated carbon can absorb it either physically or chemically. In the presence of oxygen, nonspecific physisorption using weak van der Waals interactions can convert H_2S to elemental sulphur or sulphur oxide, whereas chemisorption of H_2S by functional groups present on the AC can convert it to elemental sulphur or sulphur oxide. The surface chemistry of activated carbons, which was initially linked to the concentration of ash and some elements present such as oxygen, nitrogen, and sulphur, is strongly influenced by their adsorption capacity. Apart from hydroxyl groups, other oxygen functional groups such as pyrone, carbonyl, ester, and carboxyl are active sites for H_2S removal.

H_2S can react directly with carbonyl oxygen atoms in these oxygen groups leading to the formation of C-S, C-OH, and C-SH species. The acid-base characteristics of oxygen groups are responsible of their reactivity for H_2S adsorption.

The direct adsorption of H_2S on the carbon surface was found to be based on a dissociative process and chemisorption after studying the adsorption mechanism of H_2S on activated carbon at the molecular level. The production of C-S, C-S-C, and C-SH was caused by the direct adsorption of H_2S molecules. The electrons of S and H atoms in molecule H_2S moved to the surface C atoms during the H_2S adsorption process. According to the findings, AC acts as a catalyst by promoting the dissociation of H_2S molecules while also providing active sites for H_2S adsorption. Surface modification of ACs can be done in a variety of ways, including using heteroatoms, chemical impregnation, and metal oxide deposition (Khabazipour & Anbia, 2019).

2.5.4. Mesoporous silica

Mesoporous silica structures are a type of silica material with unique properties such as large pore size homogeneous channels, high surface area, high porosity, narrow pore size distributions, superior mechanical and thermal stability, and customizable structure. There are several forms of mesoporous silica structures that differ in pore organization but have similar pore diameters and wall thicknesses. The flexibility to alter the size and form of the pores based on the synthesis procedure, the silica supply, and the type of surfactant used is the main advantage of these materials. As a result, various mesoporous materials have been developed, with different acronyms such as *Mobil Composite of Matter* (MCM), *Hexagonal Mesoporous Silica* (HMS), *Michigan State University* (MSU), *and Folder-Sheet Mesoporous Material* (FSM). These structures with a large number of open pores allow reactants to flow freely down the channels without blocking the pores. The frameworks of mesoporous silica materials, on the other hand, are neutral, therefore their attraction for H_2S is limited. Consequently, immobilization of active particles or the functionalization of mesoporous silica materials with active components can be interesting ways to obtain superior materials with improved desulfurization performance because they combine the physicochemical properties of the incorporated active phase with the outstanding properties of well-ordered mesoporous silica structures.

Amine modification is one method for improving the adsorption capacities of mesoporous silica structures. In general, the kind and amount of amine functionalities greatly influence the H_2S adsorption by these amine-modified mesoporous silicas (Khabazipour & Anbia, 2019).

2.5.5. Zeolite

Zeolites are porous crystalline aluminosilicates made up of a three-dimensional framework of SiO_4^{4-} and AlO_4^{5-} tetrahedral that are linked by oxygen atom bridges. The aluminosilicate structure is negatively charged due to aluminium, and the zeolite matrices include a variety of exchangeable cations (univalent or bivalent) to keep the overall framework neutral. Because typical micropore size of zeolites is similar to that of many small molecules, they are a useful material for a variety of applications, including H_2S removal. The suitability of zeolite materials for adsorption is determined by the Si/Al ratio. Lower Si/Al ratio zeolites are more hydrophilic and have a better affinity for adsorbing polar molecules like H_2S. Adsorptive desulfurization has been achieved using a variety of synthetic and natural

zeolites. The adsorptive desulfurization of zeolites has been demonstrated to be based on a physisorption or chemisorption mechanism. Sulphide-sorbent π-complexation and sulphur metal (S-M) bond formation based on direct coordinate bonding have both been proposed as processes for H_2S chemisorption. Different metal ions, such as K^+, Ag^+, Cu^+, Zn^{2+}, and Ni^{2+}, have the ability to produce π-complexation between metal ions and sulphur in zeolites (Khabazipour & Anbia, 2019).

2.5.6. Metal-Organic Frameworks

MOFs are porous materials in which metal ions or small metallic clusters are chemically coordinated to multifunctional organic ligands within a porous framework. Many MOFs have unique characteristics such as high porosity, variable pore size, huge surface area, and a wide range of metal centres and ligands, which make them excellent for gas uptake. MOFs have been extensively studied for H_2S removal in the literature, with notable results, due to the existence of metallic sites and organic ligands, which provide each unit with a possible coordination-adsorption site for H_2S capture.

MOFs can remove sulphur by a variety of mechanisms, including physisorption, chemisorption, and hydrogen binding interactions. In chemisorption, sulphur adsorption produces metallic sulphides and H_2O, which can lead the initial MOF framework to collapse. The weak contact occurs between the electron-rich framework and the electron-poor sulphur atoms in the latter process. As a result, the composition of target sulphur species as well as the structure of MOFs (e.g., framework topology, metallic cluster, and organic ligand types) are critical in defining the removal method. MOFs are rarely used in practical applications due to their high costs (Khabazipour & Anbia, 2019).

2.6. Adsorbents from lignocellulosic materials for H_2S removal

The use of lignocellulosic biomass to manufacture activated carbon is an important strategy for reducing air pollution and the re-use of waste materials. Agricultural wastes, such as lignocellulosic biomass, are plentiful. Converting these wastes into high-value products like activated carbon could help tackle environmental issues like agricultural waste accumulation, air pollution, and water contamination. Lignocellulosic biomass generated from agricultural by-products has proven to be a potential raw material for the production of activated carbon, owing to its low cost and for the great availability.

Lignocellulosic biomass is generally composed of three different components, which are cellulose, hemicellulose, and lignin. The primary component in lignocellulosic biomass that is responsible for the adsorption process has been identified as *lignin*. Due to the high carbon content of lignite, lignocellulosic materials are an excellent option for use as activated carbon precursors (Mohamad Nor et al., 2013).

Activated carbons can be made from a variety of lignocellulosic biomass sources, including hazelnut shells, almond shells, coconut shells, pistachio shells, wood, palm shells, peach stones, apricot stones, and plume stones.

To be used as activated carbon, lignocellulosic materials must undergo a carbonisation/pyrolysis process with subsequent physical or chemical activation. Chemical activation is usually done with chemicals like $ZnCl_3$, NaOH, and KOH.
Activated carbons derived from lignocellulosic materials have been used to remove a variety of gaseous pollutants, including SO_2, NOx, and, in particular, H_2S. The main materials utilized to remove H_2S by adsorption on lignocellulosic activated carbon include *red pine wood*, *palm shells*, *peach* and *apricot stones*, *coconut shells* and *pistachio shells* (Mohamad Nor et al., 2013).

For the elimination of H_2S, activated carbons deriving from coconut shells have been utilized. The adsorption capacity of these activated carbons can be improved by means of impregnation with either strongly basic compounds or oxidants. Adsorption tests carried out at low concentrations (10 ppm) and high concentrations (3000 ppm), have shown that the adsorption capacity is dependent on the number of base groups present on the surface of the materials (Elsayed et al., 2009). Another activated carbon produced from coconut shells was used for H_2S adsorption, which was wet impregnated with copper nitrate. Impregnation has boosted the material's adsorption capability when compared to the non-impregnated one (Huang et al., 2006). In addition, activated carbon deriving from coconut shells have also been tested for the desulphurisation of biogas, with an initial concentration of 2400 ppm. In this case, the material was impregnated with 2 wt.% potassium iodides (Pipatmanomai et al., 2009).

Oil-palm shells, physical activated and chemically activated by impregnation with KOH or H_2SO_4, are another lignocellulosic material used as activated carbon. It has been noted that these activated carbons performed better than the palm-shell activated carbon by thermal activation and a coconut-shell-based commercial activated carbon (Guo et al., 2007).

CHAPTER 3. MATERIALS AND METHODS

This chapter discusses the devices and equipment utilized for the precursors' preparation, the laboratory setup for producing the adsorbents employed, as well as the laboratory scale plant used for conducting experimental adsorption tests. Furthermore, the experimental methodologies employed are described, as well as the adsorbent materials employed.
The experimental campaign was carried out in the laboratories of the Department of Chemical Engineering, at "Engineering School" of the University of Seville.

3.1. Materials: precursors

The lignocellulose materials chosen as precursors are almond shells and walnut shells, being waste products of the food industry and available in large quantities, especially in Italy and Spain, because of the great production that takes place in these territories.
Starting from these precursors, twelve adsorbents were obtained by activation with heat treatments, described in the following paragraphs.

3.1.1. Precursors' preparation

Both walnuts and almonds were peeled manually to acquire the shells, which served as precursors to the adsorbents used, in order to determine the proportion of shells obtained from each nut. The percentages of shells obtained for each kilogram of almonds and walnuts are shown in **Tables 3.1** and **Table 3.2**, respectively.

Whole almond (shell and nut) [g]	Shell [g]	% (Shell/Whole almond)
999,9	768	76,81%
1000,6	772,4	77,19%
1004,3	772,9	76,96%
1000	762,1	76,21%
1027,6	787,2	76,61%
1000,8	769,3	76,87%
1000,4	765,1	76,48%
1001,1	769,8	76,90%
1000,1	768	76,79%
1025,4	790,4	77,08%

Table 3. 1 - Almond shells

Whole walnut (shell and nut) [g]	Shell [g]	% (shell/whole walnut)
1006,4	554,8	55%
1005,1	528,3	53%
1002,2	519,7	52%
1003,2	516,2	51%
1021,7	529,8	52%

Table 3. 2 - Walnut shells

A variable quantity of shells, usable as precursors for adsorbents of lignocellulosic materials, can be obtained from both fruits. In particular, the percentage of shells collected per kilogram of almonds is very high, about 77%, as shown in **Table 3.1**. According to **Table 3.2**, the percentage of walnut shells obtained is around 50% per kilogram. The shells of almonds and walnuts, without any treatment, are shown in *figure 3.1* and *figure 3.2*, respectively.

Figure 3. 1 - Almond shells

Figure 3. 2 - Walnut shells

The shells must be crushed to obtain the grain size of interest, which in this case is between 1-2.83mm. Therefore, two different mills were used: a *jaw mill* (RMU-72) for the first crushing of almond and walnut shells, and a *blade mill* (RETSH SM100) for the second crushing, aiming at getting the desired grain size.

- ***Jaw mill***

The jaw mill (*figure 3.3*) works by applying the principle of crushing by compression. The crushing of the material takes place in the conical-shaped crack between the fixed crushing jaw and the jaw moved by an eccentric shaft. The elliptical movement shatters the material, which falls by gravity. This process continues until the material becomes smaller than the crushing crack. The mill has three opening levels:

- The first allows to obtain a product with maximum grain size (75%).
- The second provides for an opening of 50%.
- The third allows us to obtain a product with the finest grain size (25%).

To obtain the product of interest, the mill was used with an opening of 25%.

Figure 3. 3 - Jaw mill (front and side view) (RMU-72)

- ***Blade mill***

The blade mill (*figure 3.4*) exploits the principle of grinding by cutting; the control of the grain size and the consequent possibility of varying the size of the final product is entrusted to the presence of a perforated sheet metal grid. The grid used in this case has a 10 mm outlet hole. The evacuation of the ground is by gravity. Granulation is accomplished by cutting the incoming material with rotor blades that are mounted to the casing and aided by the presence of counter blades at a close distance from the rotating blades.

Figure 3. 4 - Blade mill (RETSH SM100)

To sieve the product obtained from the blade mill, an *electromagnetic sieve* (RETSCH AS200) at 70% of power is used with continuous vibration for 15 minutes, so as to obtain the material with the grain size of interest.

The ***electromagnetic sieve*** (*figure 3.5*) enables for the automatic separation of material for each screen based on grain size, i.e., the determination of the dimensional assortment of the investigated sample. It uses electromagnetic pulses and is controlled by a microprocessor equipment that can do a variety of tasks, including sieving timing, vibration intensity modulation, and continuous or intermittent sieving mode adjustment. Three types of movement are possible when the various control functions are combined with the vibrating action: rotating movement, vertical movement, and lateral movement.

Figure 3. 5 - Electromagnetic sieve (RETSCH AS200)

At the exit of the electromagnetic sieve, materials with three different grain sizes are obtained (*figure 3.6),* that is:

- Dimension > 2.83 mm.
- Dimension between 1-2.83 mm.
- Dimension < 1 mm.

The material of interest has a granulometry of 1 - 2,83 mm.

Figure 3. 6 - (a) Almond shells [>2,83mm]; (b) Almond shells [1-2,83mm]; (c) Almond shells [<1mm]; (d) Walnut shells [>2,83mm]; (e) Walnut shells [1-2.83mm]; (f) Walnut shells [<1mm]

3.2. Setup for adsorbent preparation

The heat treatments, used for the production of activated carbon (thermal activation) were carried out in a *tubular furnace* (TermoLab – TH1200) operating at controlled atmosphere, in which the samples were pyrolyzed and physically activated.

Figure 3.7 shows a schematic representation of the installation used for the production of adsorbents.

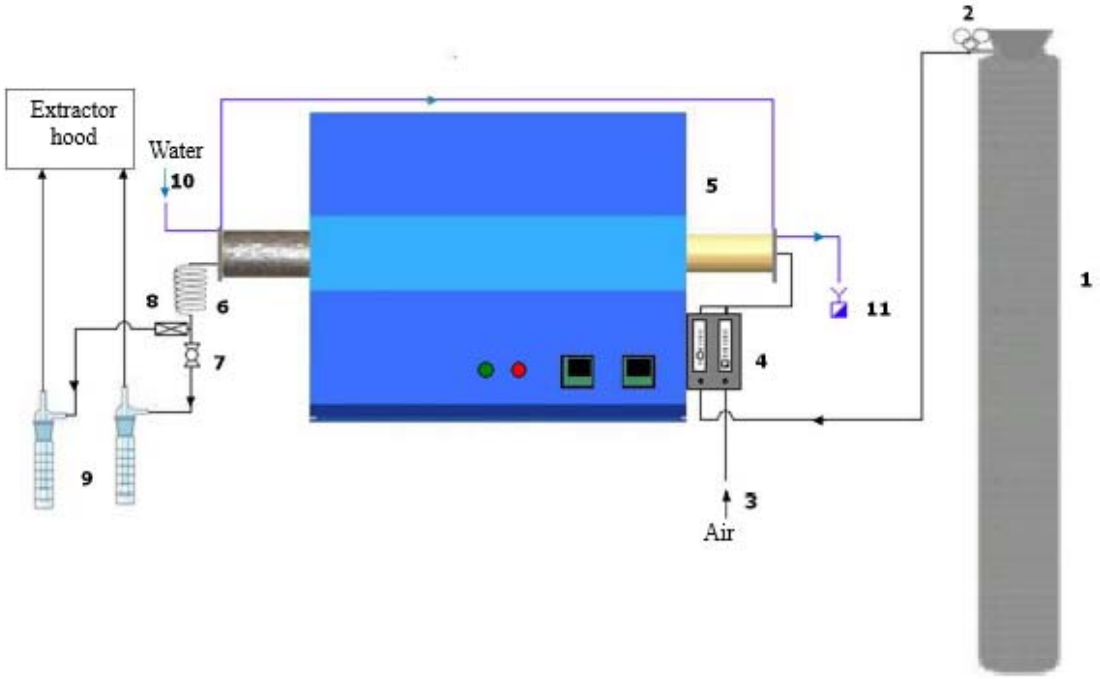

Figure 3. 7 - Adsorbent production installation diagram (Gutiérrez Ortiz et al., 2014)

The installation's numbered elements are:

1. Dry nitrogen tank
2. Pressure reducer and pressure gauges
3. Air feed
4. Gas rotameters
5. Tubular furnace
6. Copper spiral
7. Ball valve
8. Safety valve
9. Bubblers
10. Cooling water feed
11. Drain

A dry nitrogen tank (1) is used to provide the nitrogen feed, with a pressure reduction (2) reducing the bottle pressure from 200 bar to 2 bar. There are also two pressure gauges, which are used to measure the pressure in the bottle and the pressure by which the gas is fed into the system. *Figure 3.8* shows the photo of the nitrogen tank with the pressure reducer and the two pressure gauges.

Figure 3. 8 - Nitrogen tank with the pressure reducer and the two pressure gauges

Laboratory installation air is used for air feed (3). The gas rotameters (ABB) (4), which are located on the furnace's side, control the flow rate of both gases (*figure 3.9*). Two measuring ranges are available: 0-9,6 L/min and 0-1,28 L/min.

Figure 3. 9 – Rotameters

The gas enters the tubular furnace (5) through one end's steel lids and exits through the other end, through the furnace's interior. The furnace pipe is made of mullite, which is a non-porous and waterproof material.

The gases and vapours produced in the process exit the furnace and pass through a copper spiral (6) to cool before heading to two parallel bubblers (9), each filled with sunflower oil, where most of tars and heavy compounds present in the gases are removed at room temperature. A ball valve (7) is placed to lead the gases to a single bubbler or both. If a pressure of 64 mbar is exceeded, the safety valve (9) opens to prevent overpressure inside the furnace due to possible duct bottlenecks. *Figures 3.10 and 3.11* show the copper spiral, the bubble valve, the safety valve and the bubblers, respectively.

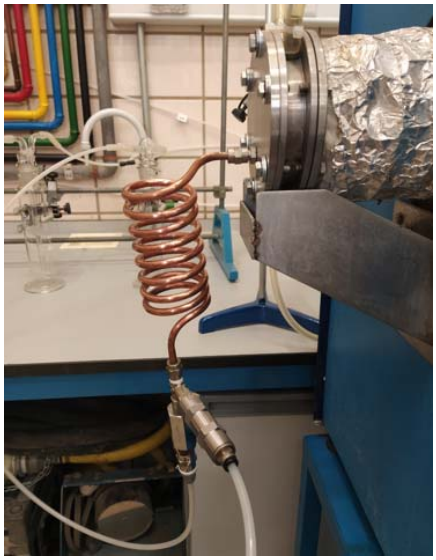

Figure 3. 10 - Furnace outlet: copper spiral, bubble valve and safety valve

Figure 3. 11 - Bubblers

The gases that escape from the bubblers' oil are sent to the atmosphere, through the extracting hood.

Using O-ring seals, the two steel lids completely seal the inside of the furnace. These must be protected from the high temperatures achieved in the furnace by a water-cooled refrigeration circuit (10-11) to lengthen their service life. For the cooling of the seals, the two lids are linked in series with a maximum water flow of 2 L/min at temperature of 20 °C.

The sample to be treated is enclosed in three ceramic capsules (*figure 3.12*), which are then placed on a refractory material plate to make insertion into the furnace and extraction easier (*figure 3.13*).

Figure 3. 12 - Samples in the capsules

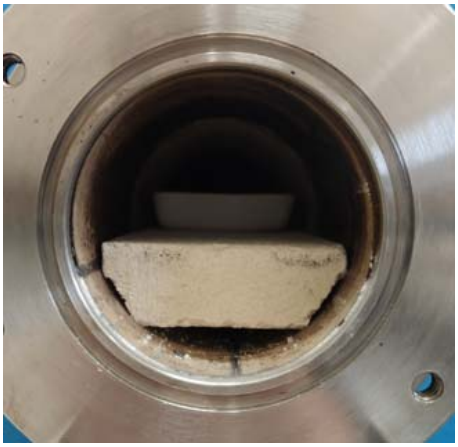

Figure 3. 13 - Insertion of the capsules in the furnace

3.2.1. Tubular furnace

A horizontal-charging tubular furnace was employed for the experiment. To operate with a regulated atmosphere, the samples are packed within ceramic capsules and placed inside a tube with dimensions 70x60x400 (ϕ_{ext}, ϕ_{int}, L) made of mullite ceramic material and lids made of stainless steel AISI 304 (*figure 3.12*).

Figure 3. 14 - Tubular furnace (TermoLab)

The furnace is programmable and may achieve a maximum temperature of 1200 °C when the heating speed is set correctly. It has a total heating length of 400 mm and two temperature control zones: a central zone of 200 mm and an area generated by the two extremes of 100mm each. The furnace has a temperature controller for the extremes and a temperature controller for the central zone, as well as two type K thermocouples in each zone, ensuring a stable temperature zone within the tube of 300 mm.

3.2.2. Experimental procedure: adsorbents production

For the production of the adsorbents, a physical activation of the precursors by heat treatments. Two samples of precursors were dried before being subjected to thermal treatments in order to measure the percentage of humidity present. The samples were warmed in a furnace to 105 °C and kept at that temperature for three hours.

The precursors have been subjected to two different thermal treatments, involving pyrolysis with N_2 up to 500 °C and subsequently a thermal activation with air at three final temperatures (500 °C, 700 °C, 900 °C).

The physical activation includes the carbonization or pyrolysis of the precursors, i.e., the conversion of the raw material into coal, and the activation of the material, i.e., the oxidation that enhances the development of the porous internal structure. Pyrolysis is carried out in an oxygen-free atmosphere from room temperature to 500 °C, with a N_2 flow rate of 1.3 L/min, allowing the release of volatile compounds from the material and resulting in a highly carbonaceous structure. The material is then activated using an air flow rate of 0.4 L/min at temperatures of 500 °C, 700 °C, and 900 °C.

In order to obtain different physical-chemical characteristics, the precursors were subjected to two different thermal treatments.

The first thermal treatment (PA-T1) involves:

1. Pyrolysis with N_2 (1,3 L/min) up to 500 °C, with a heating rate of 5 °C/min.
2. Physical activation with air (0,14 L/min) up to the final temperatures (500 °C, 700 °C, 900 °C) with a heating rate of 5 °C/min.
3. Holding time at final temperature (500 °C, 700 °C, 900 °C) with air (0,14 L/min) of 30 min.

The second heat treatment (PA-T2) involves:

1. Pyrolysis with N_2 (1,3 L/min) up to 500 °C, with a heating rate of 7 °C/min.
2. Holding time at 500°C with N_2 (1,3 L/min) of 30 min.
3. Physical activation with air (0,14 L/min) up to the final temperatures (500 °C, 700 °C, 900 °C) with a heating rate of 5 °C/min.
4. Holding time at final temperature (500 °C, 700 °C, 900 °C) with air (0,14 L/min) of 30 min.

Before beginning the thermal treatments, the two rotameters on the side of the furnace must be calibrated to determine the actual flow in L/min for each percentage number. The calibration of the two rotameters was carried out using a reference rotameter, with a nitrogen flow rate at 2 bar and a temperature of 18 ºC.

The precursors were placed into three ceramic capsules, each of which can hold roughly 15g of material, to carry out the heat treatments inside the furnace. The capsules were placed on a refractory material plate to facilitate insertion and extraction from the furnace.

The capsules were weighed before being placed in the oven, first without the solid and then totally filled with material, to determine the amount entering the oven before the heat treatments.

To perform the thermal treatments, it’s necessary to program the furnace's heating modes using the two temperature controllers, one for the central area and the other for the furnace's external sections, respectively. The samples are positioned in the furnace's approximate centre, in order to achieve and keep a consistent temperature. Once the heat treatments have been completed, the furnace is cooled to a temperature below 200 ºC, so that the samples can be extracted.

The samples are weighed at the end of the thermal treatment, once the furnace has reached ambient temperature, to determine the weight loss caused by the thermal treatment.

Each thermal treatment was repeated twice on the individual samples in order to obtain a higher quantity of adsorbent, which was sufficient for the adsorption experiments.

It is important to underline that once a material's adsorbent synthesis is complete, the tar residues must be removed from the furnace before the second material is treated. To achieve this, heating was carried out at a rate of 7 °C/min from room temperature to 850 °C, with a 60-minute holding time and an air flow of 0.2 L/min. Following the completion of the heating phase, the same air flow was circulated throughout the cooling phase until the room temperature was reached.

3.3. Laboratory scale plant for adsorption tests

In this thesis work the following adsorbent solids were generated, obtained from the thermal treatments carried out. As previously stated, the PA-T1 treatment involves pyrolysis of the precursors, AC and CN, at 500 °C with a nitrogen flow rate of 1,3 L/min; then activation at 500 °C, 700 °C, and 900 °C with an air flow rate of 0,14 L/min for 30 minutes. The PA-T2 treatment, on the other hand, provides an additional maintenance time of 30 minutes before the activation phase.

Each adsorbent is named with the acronym of their precursors (CA for almond shells - *cascara de almendras* - and CN for nut shells - *cascara de nueces*), the sample's maximum temperature, the abbreviation PA (pyrolysis and calcination/activation), and the type of treatment to which it was subjected (T1 or T2):

- *CA-500-PA-T1*, generated by precursors of almond shells, with a physical activation treatment (T1) at 500 °C.
- *CA-700-PA-T1*, generated by precursors of almond shells, with a physical activation treatment (T1) at 700 °C.
- *CA-900-PA-T1*, generated by precursors of almond shells, with a physical activation treatment (T1) at 900 °C.
- *CA-500-PA-T2*, generated by precursors of almond shells, with a physical activation treatment (T2) at 500 °C.

- *CA-700-PA-T2*, generated by precursors of almond shells, with a physical activation treatment (T2) at 700 °C.
- *CA-900-PA-T2*, generated by precursors of almond shells, with a physical activation treatment (T2) at 900 °C.
- *CN-500-PA-T1*, generated by precursors of walnut shells, with a physical activation treatment (T1) at 500 °C.
- *CN-700-PA-T1*, generated by precursors of walnut shells, with a physical activation treatment (T1) at 700 °C.
- *CN-900-PA-T1*, generated by precursors of walnut shells, with a physical activation treatment (T1) at 900 °C.
- *CN-500-PA-T2*, generated by precursors of walnut shells, with a physical activation treatment (T2) at 500 °C.
- *CN-700-PA-T2*, generated by precursors of walnut shells, with a physical activation treatment (T2) at 700 °C.
- *CN-900-PA-T2*, generated by precursors of walnut shells, with a physical activation treatment (T2) at 900 °C.

The experimental adsorption tests were carried out in a laboratory scale set up (*figure 3.15*.)

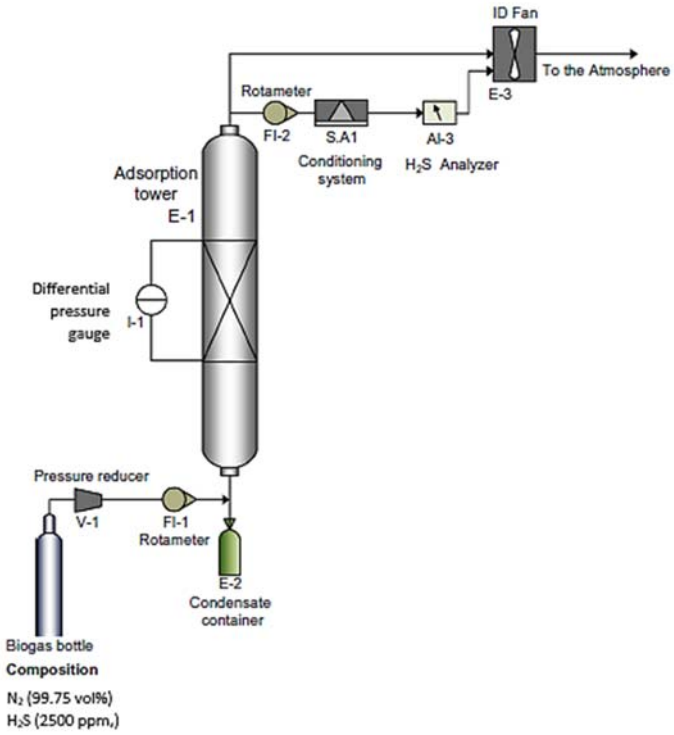

Figure 3. 15 - Scheme of the laboratory plant for performing the adsorption tests (Gutiérrez Ortiz et al., 2014).

Figure 3.16 shows an image of the whole system:

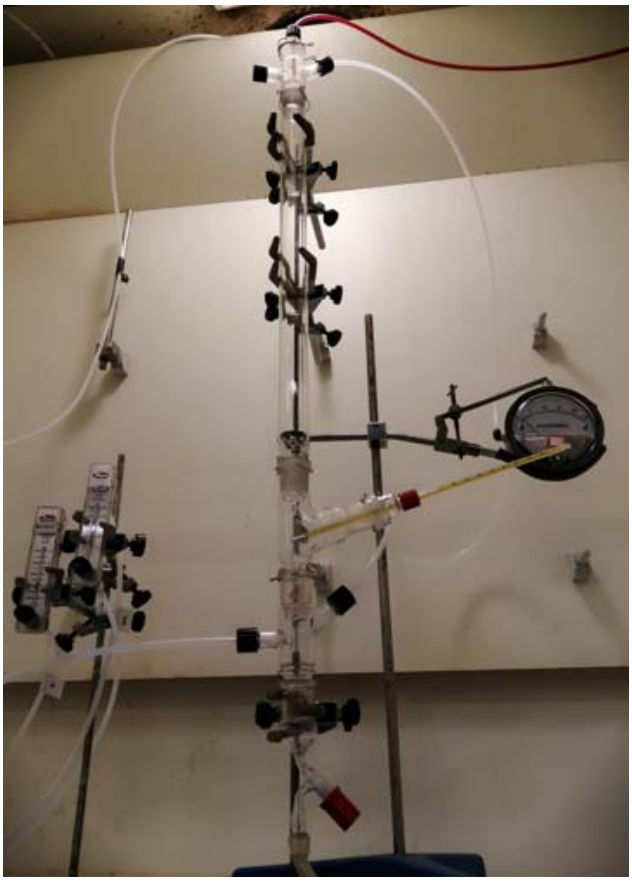

Figure 3. 16 - Adsorption plant on laboratory scale

The plant used consists of three different sections:

- Model gas supply.
- Adsorption system.
- Gas analysis system

A simulated biogas with a composition of 0.25 vol% H_2S (2500 ppm_v) in nitrogen, available as compressed gas in a tank of certified composition, was used to conduct the adsorption tests. A pressure reducer (Linde) with two manometers is arranged on the tank, allowing to measure and control the pressure inside the bottle and the pressure with which the gas is delivered into the system (*figure 3.17).*

Figure 3. 17 - Simulated biogas bottle, with pressure reducer and pressure gauges

To measure the supplied gas flow, a rotameter (Dwyer) is employed, calibrated using nitrogen at 2 bar and atmospheric temperature with a measuring range of 0.5 - 5 L/min.

The adsorption experimental reactor, which is represented by a fixed-bed column, is made up of five parts:

- A Pyrex glass adsorption column, 30 mm in diameter and 430 mm in height, where the adsorbent to be tested is placed. In the column is placed a grid to support the adsorbent, which also allows a good distribution of gas.
- A Pyrex glass sedimentation chamber at the bottom of the column, connected to a condensate container.
- A Pyrex glass chamber at the bottom of the column with two connections. The first connection, on the left side, is dedicated to gas supply to the fixed-bed column. The differential pressure gauge is attached to the second connector.
- A Pyrex glass chamber at the bottom of the column in which is placed a thermometer for measuring the temperature of the gas current.
- A Pyrex glass chamber in the top section with two connection pipes, similar to the one at bottom and with similar function. The first connection connects the adsorption column and the hydrogen sulphide analyzer. The differential pressure gauge is attached to the second connector.

The two connections at the top and bottom of the column are connected to a differential pressure gauge, which allows to measure the pressure drop in the fixed bed column.

The H_2S analysis system is allocated on the outlet line of the adsorption column and is formed by an ABB analyzer (Advance Optima AO2020 – Limas11) and an ABB conditioning system. The analyzer (*figure 3.18*) uses UV radiation to continually measure the concentration of H_2S output from the column in a range of 0 to 2500 ppmv. The air conditioning system (*figure 3.19*) runs at low temperatures to allow the gas stream to cool quickly and remove any residual humidity content that could interfere with the H_2S measurement.

Figure 3. 18 - H_2S analyzer

Figure 3. 19 - Conditioning system

3.3.1. Experimental procedure: adsorption tests

The adsorption experimental campaign was conducted with a gas flow rate of 1,1 L/min at a pressure of 1 bar and room temperature (17°C ± 4°C).

The goal of the adsorption tests is to acquire a dynamic performance analysis through the realization of breakthrough curves, from which valuable kinetic parameters for the assessment of adsorption process rates can be obtained, and the evaluation of adsorption capacity, in order to assess whether the materials can be used as efficient adsorbents for the removal of H_2S from biogas.

In order to obtain comparable experimental data, adsorbents were used in similar quantities during the conduction of the experimental tests. The quantities of adsorbents used are not

the same because of the different loss of material obtained during heat treatments. **Table 3.3** reports the weight of the adsorbent and the corresponding bed height for each produced sample.

Adsorbent	Quantity [g]	Bed height [mm]
CA-500-PA-T1	21,41	60
CA-700-PA-T1	22,99	60
CA-900-PA-T1	17,21	52
CA-500-PA-T2	22,94	72
CA-700-PA-T2	22,03	67
CA-900-PA-T2	18,53	59
CN-500-PA-T1	21,41	70
CN-700-PA-T1	22,42	69
CN-900-PA-T1	16,77	60
CN-500-PA-T2	22,94	81
CN-700-PA-T2	22,03	73
CN-900-PA-T2	15,44	58

Table 3. 3 - Quantity and bed height of the adsorbent used

The gas flow, crossing the fixed-bed column bottom-up, exiting the column is routed through an air conditioning system, which allows cooling to eliminate residual humidity before being fed to an H_2S analyzer. The ABB analyzer, model Advance Optima AO2000, measures the output concentration of H_2S continuously by ultraviolet radiation. The concentrations measured by the analyzer are reported in an Excel file, so that breakthrough curves can be obtained.

Due to the long time required, the adsorption experiments with almond shells were not carried out until the saturation, i.e., at final concentration of 2500 ppmv, while the adsorption experiments with walnut shells were carried out until the saturation.

The concentration of the adsorbate exiting the column was monitored as a function of time to determine the adsorption kinetics of H_2S. The following material balances for the adsorbed species can be used to measure the adsorption capacity, at breakpoint (3.1) and at saturation (3.2), of each dynamic test (see *section 2.3*):

$$w_{bp} = \frac{Q \cdot C_0 \cdot \int_0^{t_{bp}} \left(1 - \frac{C}{C_0}\right) dt}{m} \quad (3.\ 1)$$

$$w_{sat} = \frac{Q \cdot C_0 \cdot \int_0^{t_{sat}} \left(1 - \frac{C}{C_0}\right) dt}{m} \quad (3.\ 2)$$

In the equations (3.1) and (3.2), Q is the gas volumetric flow rate [m^3/s], C_0 the system input concentration excreted in mg/m^3, m is the adsorbent mass used [g], t_{bp} and t_{sat} are the breakpoint time and saturation time respectively, expressed in seconds. The breakpoint refers to the time for which the legal limit concentration is reached, which is 150 $\mu g/m^3$.

The resolution of the integral in equations (3.1) and (3.2) was obtained numerically by applying the *trapezium rule* to the experimental dynamic data (breakthrough curve), inserting the latter in an Excel spreadsheet.

Knowing the adsorption capacity at the breakpoint (w_{bp}) and the saturation adsorption capacity (w_{sat}), the unused bed length (LUB) can be calculated (3.3).

$$\frac{w_{bp}}{w_{sat}} = \frac{L - LUB}{L} \quad (3.\ 3)$$

Finally, to assess the efficiency of the tested materials, the results were compared with other lignocellulosic materials used as adsorbents for H_2S removal.

CHAPTER 4. RESULTS AND DISCUSSION

In this chapter, the results obtained from the production of adsorbents starting from the lignocellulosic materials chosen as precursors (i.e., almond shells and nut shells) are reported. Subsequently, the results of the adsorption tests on the produced adsorbents carried out with the simulated biogas and aimed at H_2S removal are analysed.

Finally, the adsorption capacity of the tested materials is compared to the corresponding figures of other lignocellulosic materials investigated in the literature, taken as a reference.

4.1. Material characterization

In this section, some of the characteristics of the materials that allow us to evaluate their behaviour in adsorption tests are reported.

Grain size

Almond shells and walnut shells were crushed to obtain a grain size included in the range of *1 - 2.83 mm.*

This size range was chosen because a smaller particle size (less than 1 mm) would result in a higher pressure drops due to the reduction of interparticle space; on the contrary, a bigger particle size would result in a smaller external surface, thus leading to a lower adsorption capacity.

Humidity

To determinate the humidity content in the almond shells and walnut shells, a sample of 1g of each precursor was heated in a furnace at 105 °C for 3 h. The percentage of humidity in almond and walnut shells is shown in the **Table 4.1**.

	Humidity [%]
Almond shells	11,16
Walnut shells	5,43

Table 4. 1 - Almond and walnut shells' humidity content

Almond shells have a higher percentage of humidity, which determines a lower yield.

Loss of mass and volatile matter

For the adsorbent production, the precursors were pyrolyzed at 500 °C and then physically activated at three different temperatures. The mass loss varied depending on the physical activation temperature and the material being treated. By subtracting the moisture content from the overall mass loss, the loss of volatile material may be calculated. *Figure 4.1* shows the mass-loss and the loss of volatiles for almond shells; *figure 4.2* shows the mass-loss and the loss of volatiles for walnut shells.

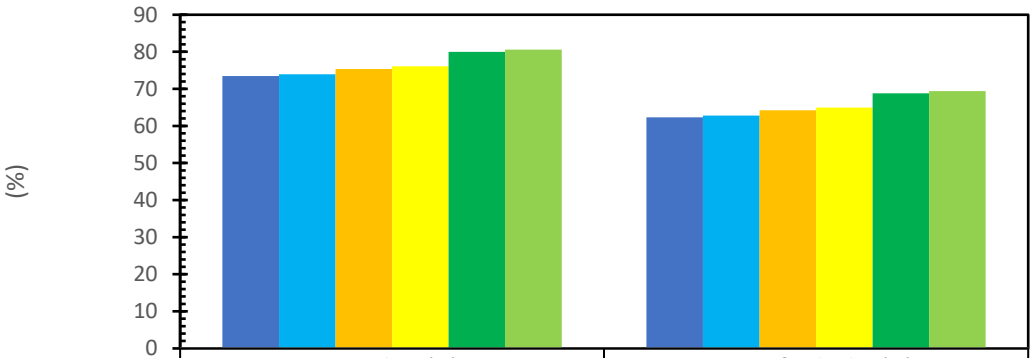

	Mass-loss (%)	Loss of Volatiles (%)
CA-500-PA-T1	73.47	62.31
CA-500-PA-T2	73.93	62.77
CA-700-PA-T1	75.37	64.21
CA-700-PA-T2	76.10	64.94
CA-900-PA-T1	79.96	68.8
CA-900-PA-T2	80.56	69.4

Figure 4. 1 - Mass-loss and loss of volatiles for adsorbents deriving from almond shells

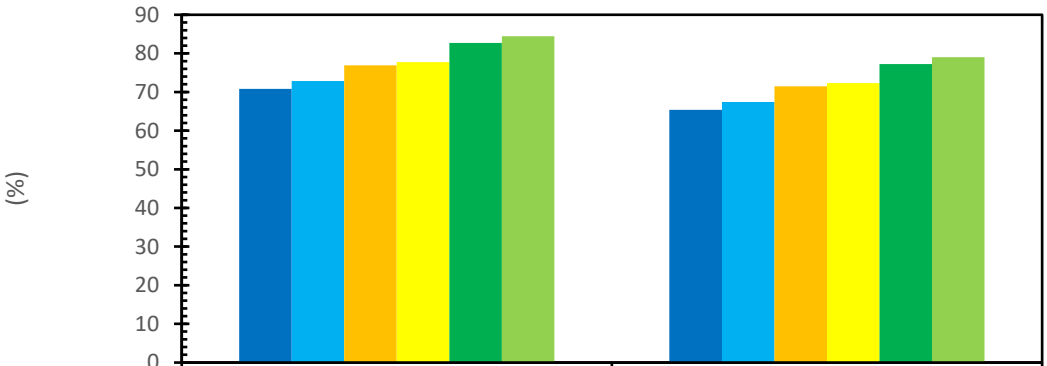

	Mass-loss (%)	Loss of Volatiles (%)
CN-500-PA-T1	70.81	65.38
CN-500-PA-T2	72.86	67.43
CN-700-PA-T1	76.91	71.47
CN-700-PA-T2	77.73	72.29
CN-900-PA-T1	82.69	77.25
CN-900-PA-T1	84.44	79.01

Figure 4. 2 - Mass-loss and loss of volatiles for adsorbents deriving from walnut shells

As expected, the mass loss of materials increases as the temperature rises. This is due to the loss of volatile substances caused by the thermal treatment of the almond and walnut shell's major constituents, i.e., cellulose (a long polymer of glucose with no ramifications) and hemicellulose (consisting of various branched saccharides). On the contrary, the third component of the shells, lignite, remains stable due to its more difficult decomposition (Omri et al., 2013). The two thermal treatments caused almost the same mass loss in almond shells; however, the T2 treatment generates a higher mass loss in walnut shells due to the additional holding time in the pyrolysis phase.

Yield

By evaluating the mass loss due to the thermal treatment, it is possible to calculate the yield of materials, which is defined as the ratio of the mass of activated carbon produced to the amount of raw material consumed (*figure 4.3* and *figure 4.4*).

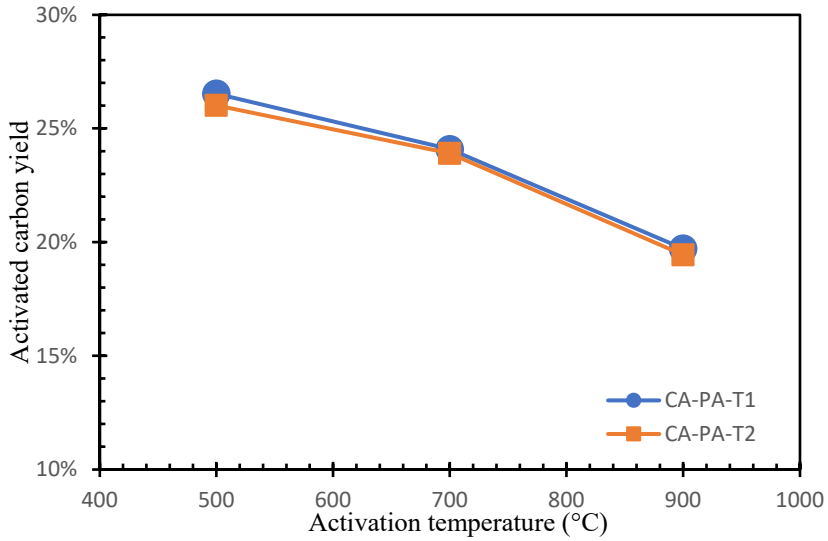

Figure 4. 3 - Effect of activation temperature on the yield of activated carbon from almond shell.

The decrease in yield is due to the increased quantity of volatile material produced by the degradation of cellulose and hemicellulose as the activation temperature rises from 500 °C to 900 °C. In particular, it is noted that the thermal treatment PA-T2 produces activated carbon with a lower yield (most for walnut shells); this may be due to the pyrolysis process, which is longer than the treatment PA-T1, thus causing greater decomposition of hemicellulose and cellulose.

Compared to adsorbents generated by almond shells, yields of adsorbents from walnut shells are slightly lower, resulting in a greater material loss. This may be justified by the fact that almond shells have a lower lignin content than almond shells (walnut shell: 18.2 % - almond shell: 27% (Caballero et al., 1996)), compared to other lignocellulosic components. Lignin, being a compound difficult to degrade, remains stable even at high activation temperatures, As opposed to the other components that are degraded, resulting in a greater loss of mass.

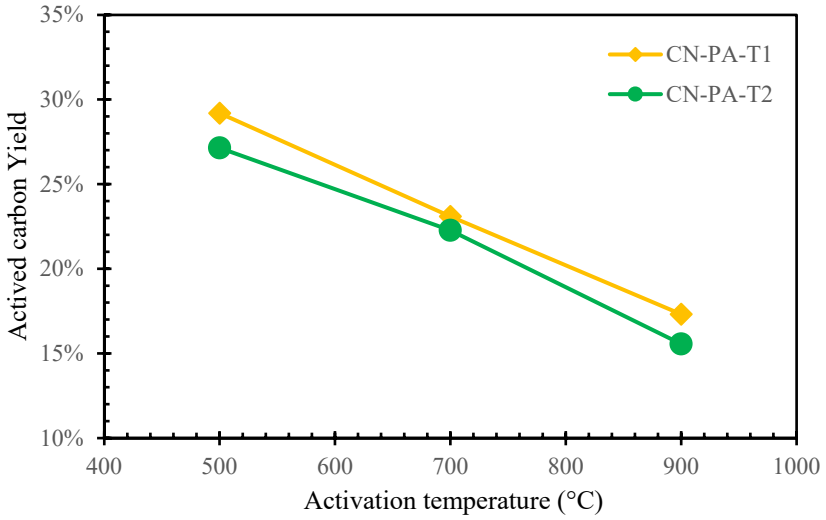

Figure 4. 4 - Effect of activation temperature on the yield of activated carbon from walnut shell

Bulk density

The bulk density (*figure 4.5* and *figure 4.6*) was determined using a calibrated cylindrical tube, which allowed the calculation of the volume occupied by the solid inside the adsorption column. Its value is also influenced by particle porosity and, hence, is linked to the activation process.

Bulk density decreases as the activation temperature increases. Considering that bulk density depends on the material porosity, a lower bulk density indicates a greater porosity. Adsorbents activated at 900°C have a reduced bulk density, likely implying a greater porosity. Furthermore, it is possible to note that materials activated by the T2 thermal treatment have lower bulk densities, which likely indicates that more porosity is formed.

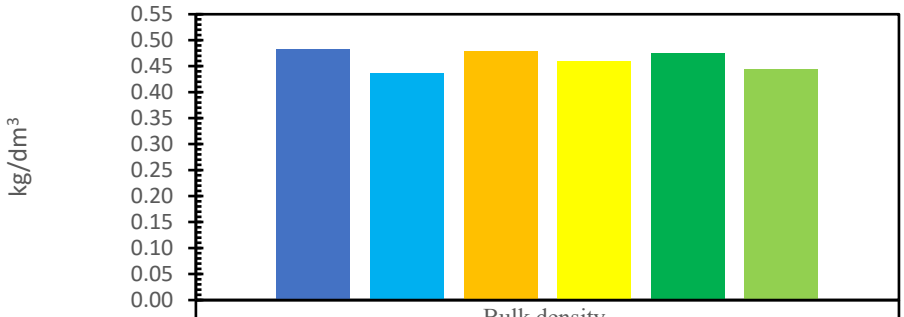

	Bulk density
CA-500-PA-T1	0.482
CA-500-PA-T2	0.436
CA-700-PA-T1	0.478
CA-700-PA-T2	0.459
CA-900-PA-T1	0.475
CA-900-PA-T2	0.444

Figure 4. 5 - Bulk density of adsorbents deriving from almond shells

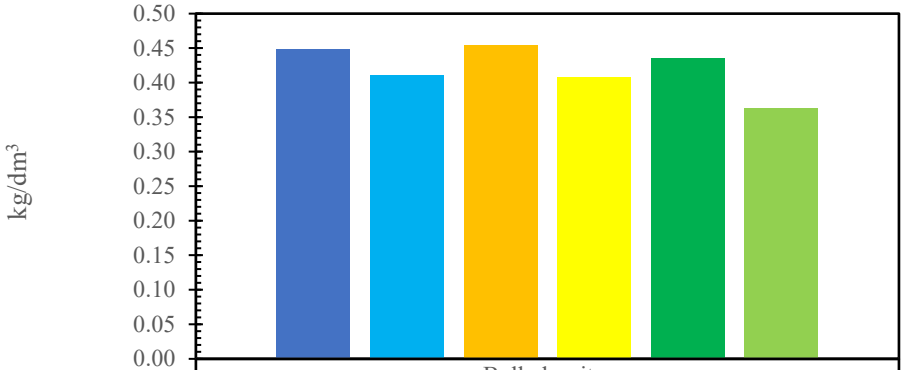

	Bulk density
CN-500-PA-T1	0.448
CN-500-PA-T2	0.411
CN-700-PA-T1	0.454
CN-700-PA-T2	0.408
CN-900-PA-T1	0.435
CN-900-PA-T2	0.363

Figure 4. 6 - Bulk density of adsorbent deriving from walnut shells

4.2. Adsorption tests

Adsorption tests were carried out using the adsorbents generated by the thermal treatments PA-T1 and PA-T2 (see *section 3.2.2*); a total of twelve distinct adsorbent was tested.

The adsorption tests were performed with a dry simulated biogas, as indicated in *section 3.3.*

4.2.1. Breakthrough curve: adsorbents deriving from almond shells

The breakthrough curves of the adsorbents produced from almond shells subjected to two thermal treatments (see *section 3.2.2*), at room temperature and at atmosphere pressure, were obtained using the experimental procedure described in *Chapter 3*.

Figure 4.7 shows the breakthrough curves of adsorbents produced by the PA-T1 treatment; *figure 4.8* shows the breakthrough curves of adsorbents produced by the PA-T2 treatment.

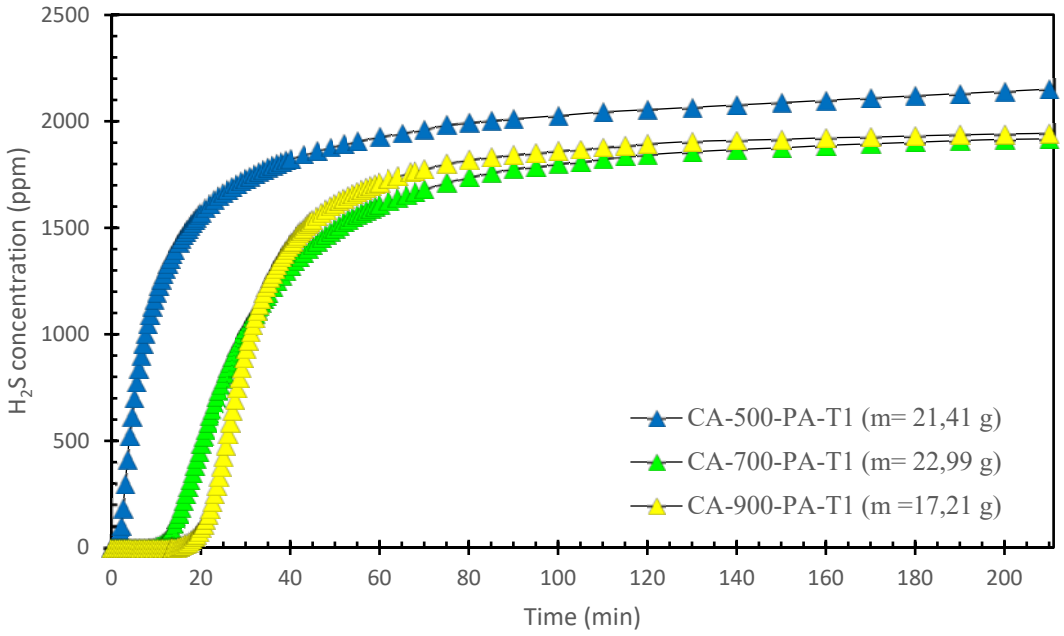

Figure 4. 7 - H_2S Breakthrough curves for adsorbents derived from almond shells, obtained by PA-T1 thermal treatment. H_2S initial concentration = 2500 ppm; T=18 °C; P= 1 atm.

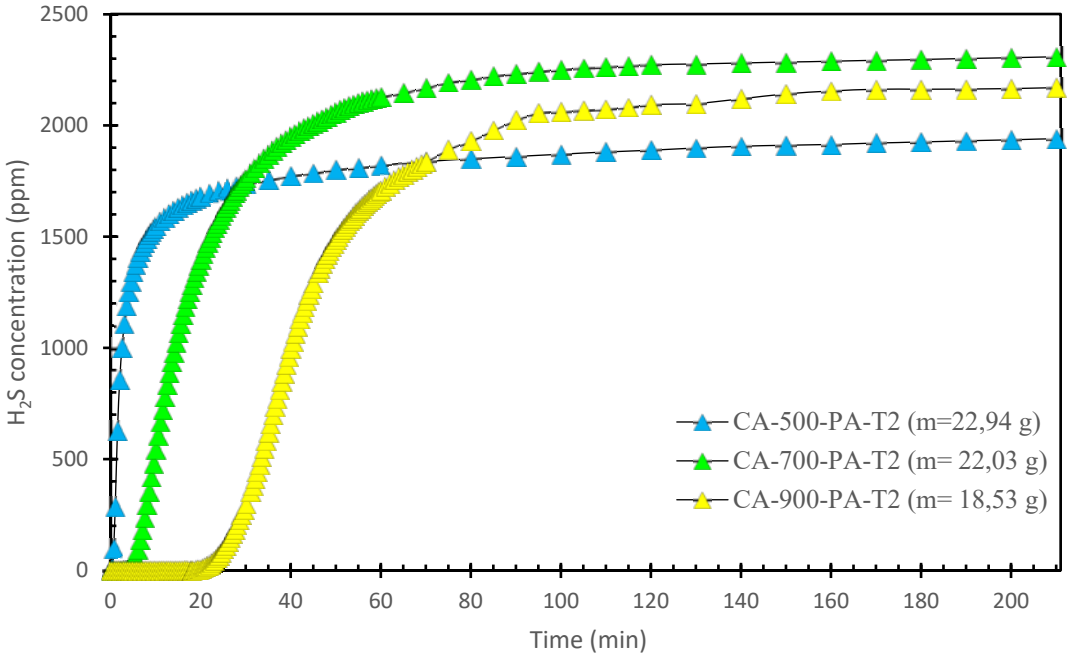

Figure 4. 8 - H_2S Breakthrough curves for adsorbents derived from almond shells, obtained by PA-T2 thermal treatment. H_2S initial concentration= 2500 ppm; T = 15± 2°C; P= 1 atm.

The adsorption runs with the adsorbents deriving from almond shells were carried out up to a time of 210 minutes. As shown in *figure 4.7* and *figure 4.8*, the adsorbents show a sigmoidal trend typical of the curves of breakthrough. In particular, for all the adsorbents, after the

ascending branch of the breakthrough curves, a plateau was reached. The occurrence of this plateau suggests the presence of a catalytic reaction during H_2S elimination via dissociative adsorption and oxidation since a pseudo-steady state is observed without the saturation of ACs. This behaviour is consistent with the finding of several works available in the literature (Ayiania et al., 2019; Bak et al., 2019; Sitthikhankaew et al., 2014). The products of catalytic reactions (elemental sulphur) are retained on the surface of the adsorbents (Surra et al., 2019a). The curves reveal that adsorption and catalysis are taking place when the steady state is reached. This indicates that the almond shell adsorbents' adsorption capacity was saturated, and that some of the H_2S was removed through a catalytic reaction. This catalytic reaction was discovered to be oxygen and carbon dependent, and to be significantly faster in the presence of water. In addition, the reaction has been discovered to occur specifically on materials with micropores (Meeyoo et al., 1997).

Similar results were also obtained for other adsorbents derived from lignocellulose materials for the H_2S removal, e.g., *Surra et al*. (2019) investigated adsorbents derived from corn cob waste impregnated with digested liquid. These materials were compared to the same ones but just physically activated. The latter did not show this behaviour, likely due to a higher ash content, a lower oxygen content, a lower micropore volume and a smaller surface area. This trend was also seen in a commercial activated carbon (CAC) specifically intended for biogas purification. Also in this case, the CAC was characterized by a high amount of Ca, Al, and Fe, all of which are known to have catalytic activities in the elimination of H_2S (Surra et al., 2019b).

Due to the occurrence of simultaneous adsorption/catalysis phenomena, the saturation adsorption capacities were not assessed; so, the H_2S adsorption capacities were calculated at *breakpoint*. For the same reason, it was not possible to evaluate the unused bed length (LUB); however, it is possible to assess the slope of the breakthrough curves to determine the system's efficiency. A steeper curve implies a more efficient system, since it allows for better utilization of the bed and hence a decrease of the unused bed. The difference between the times of two points on the curve can be used to compute the curve's slope. In this scenario, the two times considered were C/C_0=0.01 (25 ppm) and C/C_0=0.7 (1750 ppm), respectively, to define the slope of the breakthrough curves.

In order to establish a suitable comparison for the adsorbents' performance, **Table 4.2** shows the kinetic parameters that can be obtained, i.e., the breakpoint time t_s, the adsorption capacity at breakpoint w_{bp}, the time difference between the two distinct points of the curve previously defined (C/C_0=0.01 and C/C_0=0.7) Δt, in order to assess the steepness of the curve. The mass used during adsorption experiments is also reported, which differs from trial to experiment due to mass loss caused by heat treatments. Heat treatments at 900 ºC caused a greater loss of mass, resulting in a lower amount of adsorbent. It's essential to report this value because it's used in the adsorption capacity calculation (*equation 3.1*).

	m [g]	***Breakpoint* time [s]**	**w_{bp} [mg/g]**	**Δt [min]**
CA-500-PA-T1	21.41	60.2	0.18	31.14
CA-700-PA-T1	22.99	513.2	1.43	71.06
CA-900-PA-T1	17.21	813.2	3.04	47.98
CA-500-PA-T2	22.94	0.35	0.001	33.67
CA-700-PA-T2	22.03	151.6	0.45	24.82
CA-900-PA-T2	18.53	1083.1	3.84	40.81

Table 4. 2 - Kinetic parameters for adsorbents deriving form almond shells

The dynamic results reveal a significant difference in adsorbent performance depending on the temperature at which they were activated. Adsorbents activated at 900 °C have significantly longer breakpoint times than those activated at 500 °C.

Figure 4.9 shows a histogram of the adsorption capacity at breakpoint (w_{bp}) of the adsorbents utilized.

It's possible to notice how the adsorption capacity of materials increases as the activation temperature rises. In particular, physically activated carbon at temperature of 500°C have essentially negligible adsorption capacity, whilst those activated at 900°C reveal the highest adsorption capacity. This could be attributed to the volume of the pores that grows during the thermal treatments, which is minimum for the adsorbent activated at 500°C. As the treatment temperature rises, the B.E.T. surface expands, resulting in increased adsorption capacity (Gutiérrez Ortiz et al., 2014).

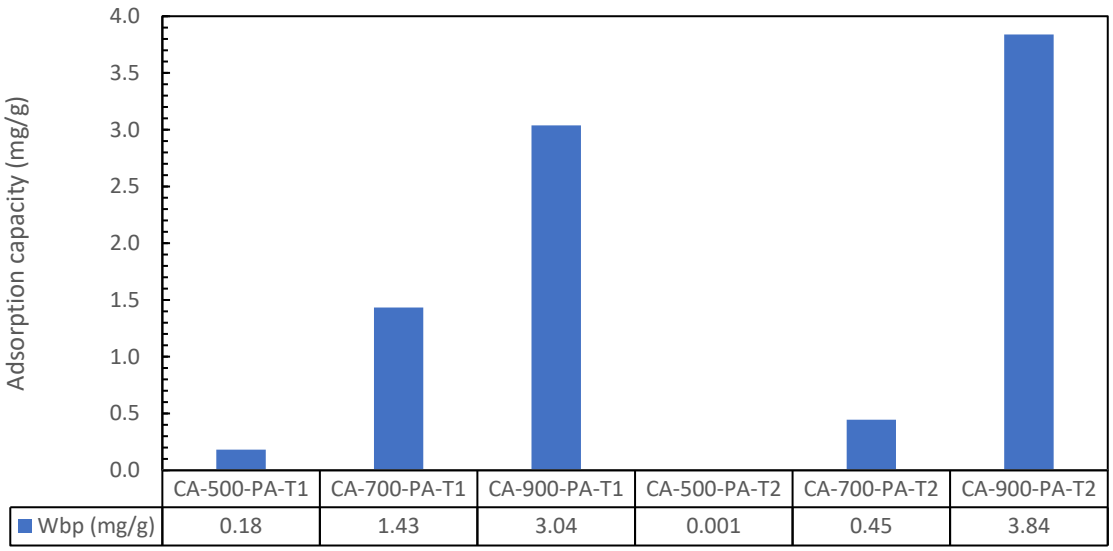

Figure 4. 9 - Breakpoint adsorption capacities for almond shell adsorbents

As a result, the activation temperature has a significant impact on the surface as well as the nature of porosity. In fact, when the temperature rises, the number of volatiles released increases as well. Higher activation temperature promotes micropores and mesopores formation, resulting in increased adsorption capacity.

In the end, as can be seen from *figures 4.7* and *figure 4.8* and **Table 4.2**, the temperature at which the highest results are obtained is 900 ºC. At this temperature, the PA-T2 thermal treatment is preferable because the sample is characterized by a longer breakpoint time and a higher adsorption capacity.

4.2.2. Breakthrough curves: adsorbents deriving from walnut shells

The breakthrough curves of the activated carbons generated from walnut shells, which were physically activated by two thermal treatments (see *section 3.2.2*), were obtained at room temperature and atmosphere pressure using the experimental procedure described in *section 3.3.1*. The breakthrough curves of the adsorbents generated according to the thermal treatment PA-T1 are shown in *figure 4.10*, while *figure 4.11* shows the breakthrough curves of the adsorbents generated according to the treatment PA-T2.

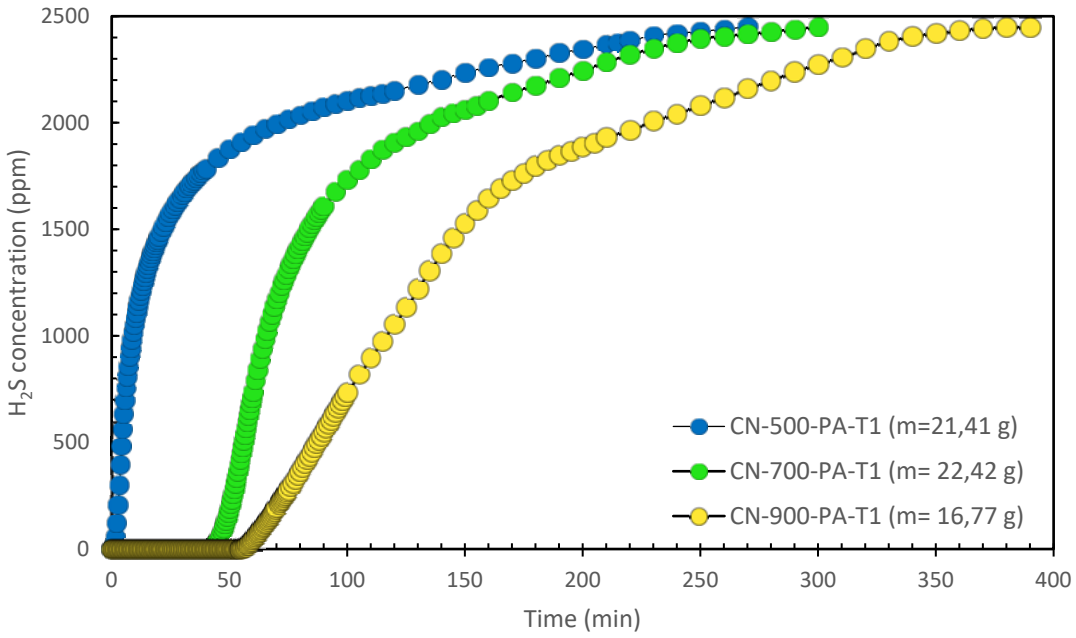

Figure 4. 10 - H_2S Breakthrough curves for adsorbents derived from walnut shells, obtained by PA-T1 thermal treatment. H_2S initial concentration = 2500 ppm; T= 19 ± 1 °C; P = 1 atm.

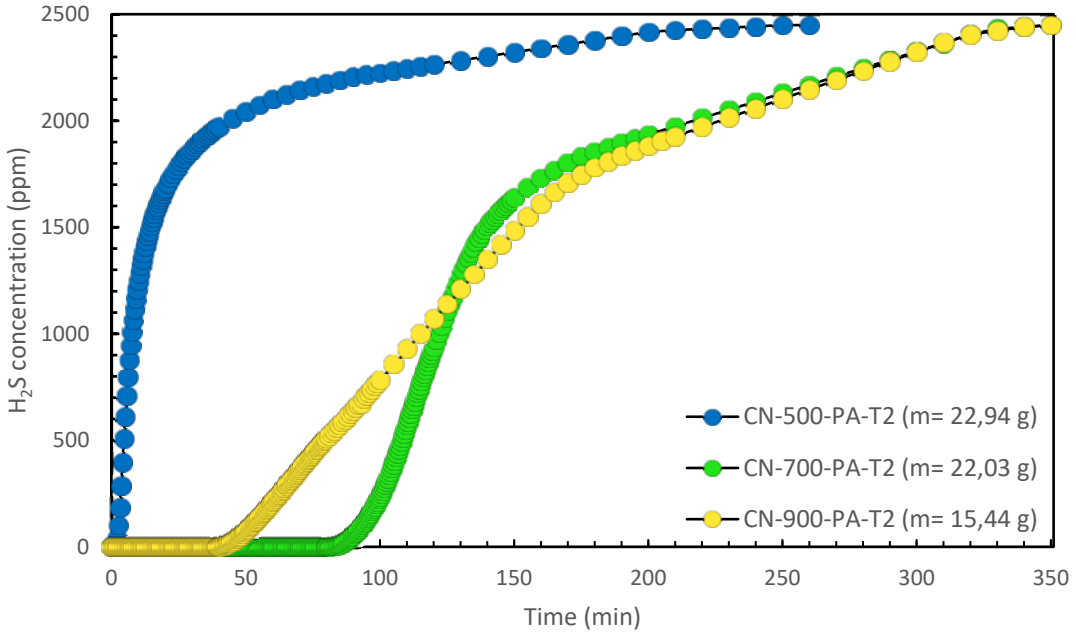

Figure 4. 11 - H_2S Breakthrough curves for adsorbents derived from walnut shells, obtained by PA-T2 thermal treatment. H_2S initial concentration = 2500 ppm; T = 20 °C; P = 1 atm.

In order to compare the performances of the various adsorbents, the different kinetic parameters are compared, i.e., breakpoint time t_s, saturation time t_{sat}, adsorption capacity at breakpoint w_{bp}, adsorption capacity at saturation w_{sat} and length of unused bed (LUB/L), set out in **Table 4.3**. Saturation time and saturation adsorption capacity were evaluated at a

$C/C_0=0.95$ ratio. The mass used during adsorption experiments is also reported, which differs from trial to experiment due to mass loss caused by heat treatments. Heat treatments at 900 ºC caused a greater loss of mass, resulting in a lower amount of adsorbent. It's essential to report this value because it's used in the adsorption capacity calculation (*equations 3.1* and *3.2*).

	m [g]	**t_s [s]**	**t_{sat} [min]**	**w_{bp} [mg/g]**	**w_{sat} [mg/g]**	**LUB/L [%]**
CN-500-PA-T1	21.41	0.5	215	0.001	7.48	99.98
CN-700-PA-T1	22.42	2433.22	240	6.99	16.77	58.34
CN-900-PA-T1	16.77	3271.8	330	12.43	35.23	64.71
CN-500-PA-T2	22.94	60.3	180	0.17	5.35	96.87
CN-700-PA-T2	22.03	4803.2	310	13.94	27.45	49.21
CN-900-PA-T2	15.44	2373.2	310	9.86	37.53	73.73

Table 4. 3 - Kinetic parameters for adsorbents deriving form walnut shells

The performance of adsorbents varies significantly depending on the temperature at which they were activated, according to dynamic data. As previously stated, walnut shells activated at 500°C have extremely short breakpoint times, resulting in reduced breakpoint adsorption capacity. For PA-T1 treatment, the adsorbent activated at 900°C has the highest adsorption capacity but uses a smaller fraction of the bed than the one activated at 700°C. The slope of the breakthrough curves, which is greater for adsorbents activated at 700°C, also indicate a faster adsorption, likely due to a greater average pore size. For PA-T2 treatment, considering the adsorption capacity at saturation, the adsorbent activated at 900°C has the maximum value. However, it is important to note that the adsorption tests were performed at different masses, and the adsorption capacity is calculated per unit mass of adsorbent; as a result, the sample CA-900-PA-T2 has the lowest mass, resulting in a greater adsorption capacity. On the contrary, in terms of application, the adsorption capacity at breakpoint is more relevant, and the sample activated at 700 °C has the higher adsorption capacity. Furthermore, CA-700-PA-T2 shows the best use of the system, with a less fraction of bed unused. In fact, in order to have an efficient system, the fraction of unused bed must be as low as possible, so that the material used is maximized.

In conclusion, the activated material at 700 °C offers a better performance, in terms of higher adsorption capacity at breakpoint, a better use of the adsorption bed and a steeper slope of the curve.

The adsorption capacities at breakpoint and saturation are reported in a histogram, shown in *figure 4.12*.

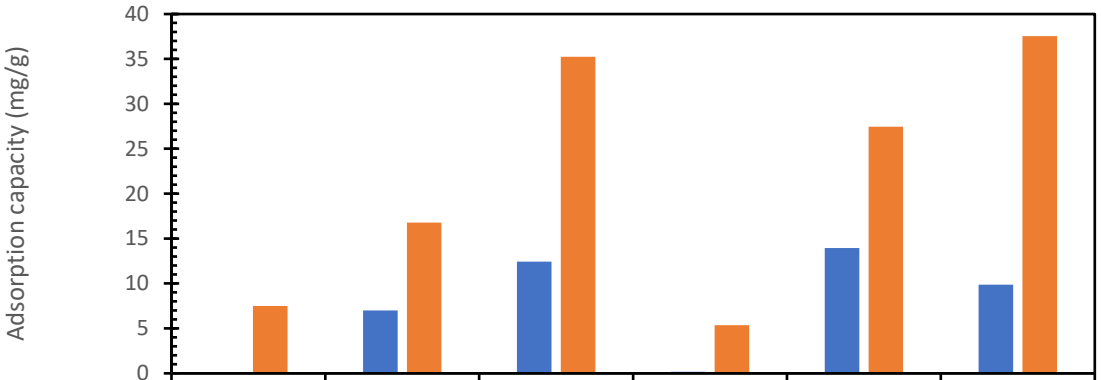

	CN-500-PA-T1	CN-700-PA-T1	CN-900-PA-T1	CN-500-PA-T2	CN-700-PA-T2	CN-900-PA-T2
Wbp (mg/g)	0.001	6.99	12.43	0.17	13.94	9.86
W sat (mg/g)	7.48	16.77	35.23	5.35	27.45	37.53

Figure 4. 12 - Adsorption capacities for walnut shell adsorbents

Walnut shells, in general, have a low ash level, a high carbon content, and a high content of volatile compounds, making them well-suited for usage as adsorbents (Kambarova & Sarymsakov, 2008). The adsorption capacity of walnuts shells increases as the activation temperature rises. This is likely due to a larger pore volume and the removal of volatile compounds. As a result, an activation temperature of 500°C is too low, as it prevents the material's porosity from developing properly, resulting in a limited adsorption capacity. Instead, the activation temperature of 900 °C allows for more micropore formation and hence more surface area (Albatrni et al., 2022). The low lignin level (18.2%) in the shells of walnuts also contributes to the development of micropores; in fact, materials with a lower content of lignin tend to produce activated carbon mostly microporous (González et al., 2009). Despite this, the optimal activation temperature appears to be 700 °C, because this temperature promotes the growth of micropores and mesopore, which allow H_2S molecules to deposit on the surface without diminishing the active surface area, resulting in a more efficient and quicker adsorption process (Gutiérrez Ortiz et al., 2014).

4.3. Comparison analysis of adsorbents performance

Based on the experimental data presented in the previous paragraph, a comparison of the performance of the adsorbents used may be made.

The results of the experimental adsorption tests are reported in **Table 4.4** in order to understand the differences between the adsorbents utilized and to determine which of them gives the best performance in H_2S adsorption for a prospective future application.

	m [g]	t_{bp} [s]	w_{bp} [mg/g]	w_{sat} [mg/g]	Δt [min]	LUB/L [%]
CA-500-PA-T1	21.41	60.2	0.18	-	31.41	-
CA-700-PA-T1	22.99	513.3	1.43	-	71.06	-
CA-900-PA-T1	17.21	813.2	3.04	-	47.98	-
CA-500-PA-T2	22.94	0.35	0.001	-	33.67	-
CA-700-PA-T2	22.03	151.6	0.45	-	24.82	-
CA-900-PA-T2	18.53	1083.1	3.84	-	40.81	-
CN-500-PA-T1	21.41	0.5	0.001	7.48	35.51	99.98
CN-700-PA-T1	22.42	2433.22	3.99	16.77	57.56	58.34
CN-900-PA-T1	16.77	3271.8	12.43	35.23	114.4	64.71
CN-500-PA-T2	22.94	60.3	0.17	5.35	21.17	96.87
CN-700-PA-T2	22.03	4803.2	13.94	27.45	75.43	49.21
CN-900-PA-T2	15.44	2373.2	9.86	37.53	130.4	73.73

Table 4. 4 - Summary table of the performance of the activated carbons used

The table demonstrates that the adsorbents obtained from walnut shells outperform those derived from almond shells for the majority of the kinetic parameters analyzed. Because the almond shells did not attain saturation, the percentage of bed used could not be calculated. Almond shell-adsorbents have shorter breakpoint times, resulting in lower adsorption capacities (at breakpoint). The best results were achieved by the adsorbent activated at 900°C, with a breakpoint capacity of 3.04 mg/g for CA-900-PA-T1 and 3.84 mg/g for CA-900-PA-T2, respectively.

The best adsorption capacity at saturation was found for walnut shells activated at 900°C, with values of 35.23 mg/g for CN-900-PA-T1 and 37.53 mg/g for CN-900-PA-T2.
Despite this, compared to the sample activated at 900 °C, the sample activated at 700 °C by T2 thermal treatment had a lower adsorption capacity at saturation but a higher adsorption capacity at breakpoint, equal to 13.94 mg/g, which makes it more useful from an application standpoint. In addition, the adsorbent activated at 700 °C shows a faster kinetic, resulting in increased system efficiency.
As a result, the adsorbent CA-700-PA-T2 offers an excellent balance of separation performance and process kinetics, making it the sorbent best suitable for the adsorption of H_2S from biogas among those tested.

4.4. Comparison with other adsorbents

In order to assess whether activated carbons from walnut and almond shells can be used for adsorption of H_2S, the performances were compared with those obtained with other materials available in the pertinent literature. Several lignocellulosic materials have been employed to produce adsorbents for the removal of H_2S, including *pistachio shells*, *coconut shells*, and *wood*; moreover, different organic waste materials have been used as activated carbon precursors for H_2S elimination, like *maize cob waste* and *coffee industry waste materials*. The comparison was made by evaluating the adsorption capacities at the breakpoint, which are of interest for a practical application of H_2S removal from biogas.

Table 4.5 shows the adsorption capacities at breakpoint obtained for different adsorbents, the breakpoint concentration at which they were calculated, and the corresponding bibliographical references.

Only those activated at 900 °C among the adsorbents produced from *almond shells* outperform some of the previously described active carbons, i.e., C-2 and MCW(PA)2h. While they perform poorly in comparison to all other adsorbents described, this implies that they are not suitable materials for H_2S adsorption.

On the contrary, the adsorbents derived from the *walnut shells*, in particular activated at 700 °C and 900 °C, offer good adsorption capacities, comparable or higher than those shown in **Table 4.5**. This advantage is reinforced when production costs are considered, as they were thermally activated using air rather than CO_2. Furthermore, for walnut shells, the best adsorption capacity at breakpoint is achieved by the activated adsorbent at 700 °C, lower

temperature than the activation temperatures of other materials; hence, it also offers an energy advantage.

	Adsorptive capacity at breakpoint [mg/g]	Breakpoint concentration	Reference
WV	17.9	100 ppm	Nguyen-Thanh & Bandosz, 2005
PC5PA	7.1	100 ppm	Bazan-Wozniak et al., 2017
PC7PA	10.5	100 ppm	Bazan-Wozniak et al., 2017
C-1	14.6	100 ppm	Elsayed et al., 2009
C-2	4.2	100 ppm	Elsayed et al., 2009
C-3	33.4	100 ppm	Elsayed et al., 2009
MCW(PA)2h	0.65	50 ppm	Surra et al., 2019
MCW(PA)3h	15.5	50 ppm	Surra et al., 2019
CP5PA	9.3	100 ppm	Nowicki et al., 2014
CP8PA	12.8	100 ppm	Nowicki et al., 2014
CA-900-PA-T2	3.84	200 ppm	This work
CN-700-PA-T2	13.94	200 ppm	This work

Table 4. 5 - Adsorptive capacity for activated carbons take as reference

WV, C-1, C-2, C-3 are commercial activated carbon derived from wood and coconut shells, respectively, used for biogas desulphurisation.

PC5PA and PC7PA are adsorbents derived from pistachio shells, subjected to physical activation. In particular, they were pyrolyzed at two temperatures (500 °C and 700 °C) using N_2, and physical activated at 900 °C with CO_2.

MCW(PA)2h and MCW(PA)3h were produced by maize cob waste. The materials were subjected to pyrolysis at 500 ºC with N_2; subsequently physically activated with CO_2 at 800 °C, for 2h and 3h.

CP5PA and CP8PA are derived from coffee industry waste materials. They were subject to a pyrolysis at two temperatures (500 °C and 800 °C) with Argon, and then physical activated at 800 °C with CO_2.

In conclusion, considering the different materials found in the literature, the activated carbons derived from walnut shells offer good adsorption capacity and lower production costs, resulting in potential adsorbents for the removal of H_2S.

CHAPTER 5. CONCLUSIONS

The continuous increase of pollutants released to the atmosphere because of human activity, primarily related to industrial processes and energy production, causes significant environmental consequences. Despite being one of the primary contributors of greenhouse gases, the usage of fossil fuels remains the world's primary source of energy. To limit the amount of pollution released in the atmosphere, one initial step can be to replace fossil fuels with renewable energy sources, such as *biogas*.

Biogas is a biofuel that is generated through anaerobic digestion, which is a process of biological decomposition of organic substances using microorganisms that operate in absence of oxygen. Biogas has a high calorific value due to its high methane content, making it as a viable renewable fuel.

Biogas must be cleaned of some components and, optionally, subjected to an upgrade process to remove CO_2 before it can be used as a source of energy through conversion to biomethane. Among the different compounds to be removed is H_2S, which can cause substantial damage to equipment as well as generate other pollutants like SOx.

Among the various techniques of H_2S removal from biogas, adsorption is one of the most competitive desulphurisation techniques, thanks to the simplicity, flexibility, and efficiency of the process.

The most common materials used in adsorption processes are activated carbons, which are mainly produced from non-renewable and expensive raw materials such as carbon, wood, polymers and petroleum residues. Producing activated carbons from agricultural waste could be a sustainable alternative, as it could boost economic returns while also reducing pollution, e.g., by reducing waste accumulation. Due to its wide availability and low cost, lignocellulosic biomass obtained from agricultural by-products could be a suitable raw material for the production of activated carbons.

In this thesis work, the adsorption of H_2S from simulated biogas was investigated, using adsorbents made from lignocellulosic material, i.e., almond shells and walnut shells.

First, the adsorption method was deepened, focusing on both thermodynamic and kinetic analysis of the process and analyzing the operating settings that determine the equilibrium conditions. The different kinds of adsorbents materials typically used were presented, such as zeolites, porous metal oxides, mesoporous silica, MOFs and activated carbon; a literature review was then conducted on the latter, emphasizing the separation efficiency and cost-effectiveness in comparison to other materials. Furthermore, the economic, availability and sustainability advantages of using lignocellulosic materials as precursors of activated carbon were assessed, reporting the main characteristics and the different lignocellulosic materials used in the literature to produce activated carbon.

In this work, almond and walnut shell were chosen as precursors and subjected to different thermal treatments for adsorbent production. For the precursors preparation, the almond and walnut shells were crushed in two mills (jam mill and blade mill) before being sieved to obtain the grain size of interest, which was 1 – 2.83 mm.

Subsequently the precursors were physically activated to obtain twelve adsorbents; in particular, the precursors underwent two thermal treatments, including pyrolysis at 500 ºC using N_2 and physical activation with air at three final temperatures (500 °C, 700 °C, 900 °C); hence, twelve different adsorbents were produced. For physical activation, a tubular furnace was used integrated in a laboratory scale installation.

Some material characteristics, such as precursor moisture, mass loss and volatile material loss, to determinate which material offered the best yield and the apparent density of the adsorbents were evaluated.

To examine the performance of these adsorbents, an experimental campaign on the different activated carbons products was conducted. The H_2S adsorption experiments were carried out in a fixed-bed column that was integrated in a laboratory scale plant, assessing the capture performance and the process dynamics.

Experiments have revealed that the adsorbents generated from almond shells have a limited H_2S adsorption capacity; in particular, a pseudo-stationary stage has been identified for these materials, which does not lead to saturation conditions. This is likely due to catalytic reactions occurring during the removal of H_2S via dissociative adsorption and oxidation. The materials activated at 900 °C showed the highest results, likely due to the increased production of micropores.

The adsorbents produced by the walnut shells outperformed the adsorbents produced by the almond shells in terms of removal performance and adsorption capacity; moreover, they exhibited better kinetic performance as well. The best adsorption capacities at saturation were obtained for materials activated at 900 °C, CN-900-PA-T1 and CN-900-PA-T2, with values of 35,23 mg/g and 37,53 mg/g, respectively. These materials, however, show very slow kinetics and a fraction of unused bed very high. The material activated at 700 °C demonstrated the best performance, especially the T2 heat treated sample, which had the highest breakpoint adsorption capacity, a better kinetic, and a reduced proportion of unused bed. This is probably due to the higher presence of micropores and also mesopores, which allow H_2S molecules to deposit on the surface without diminishing the active surface area.

Finally, the produced adsorbents were compared with other materials found in the literature, from lignocellulosic materials and organic waste materials, in order to assess whether these offer good performance to be used for the adsorption of H_2S. The comparison confirmed that activated carbons from walnut shells activated at 700 °C offer good adsorption capacity, combined with lower production costs thanks to a lower activation temperature and air usage.

In conclusion, the results of this thesis work encourage more research into the use of adsorption techniques to remove H_2S from biogas utilizing lignocellulosic materials obtained from organic waste as adsorbents; in particular, the walnut shells activated at 700 ºC proved to be suitable for the purpose, combining the cost-effectiveness and good adsorption capacities obtained.

BIBLIOGRAPHY AND SITOGRAPHY

Albatrni, H., Qiblawey, H., & Al-Marri, M. J. (2022). Walnut shell based adsorbents: A review study on preparation, mechanism, and application. In *Journal of Water Process Engineering* (Vol. 45). https://doi.org/10.1016/j.jwpe.2021.102527

Allegue, L. B., & Hinge, J. (2014). Biogas upgrading Evaluation of methods for H2S removal. *Danish Technological Institute*, *December*.

Ayiania, M., Carbajal-Gamarra, F. M., Garcia-Perez, T., Frear, C., Suliman, W., & Garcia-Perez, M. (2019). Production and characterization of H2S and PO43− carbonaceous adsorbents from anaerobic digested fibers. *Biomass and Bioenergy*, *120*, 339–349. https://doi.org/10.1016/J.BIOMBIOE.2018.11.028

Bak, C. u., Lim, C. J., Lee, J. G., Kim, Y. D., & Kim, W. S. (2019). Removal of sulfur compounds and siloxanes by physical and chemical sorption. *Separation and Purification Technology*, *209*, 542–549. https://doi.org/10.1016/J.SEPPUR.2018.07.080

Bazan-Wozniak, A., Nowicki, P., & Pietrzak, R. (2017). The influence of activation procedure on the physicochemical and sorption properties of activated carbons prepared from pistachio nutshells for removal of NO2/H2S gases and dyes. *Journal of Cleaner Production*, *152*, 211–222. https://doi.org/10.1016/J.JCLEPRO.2017.03.114

Bhatia, S. C. (2014). Biogas. *Advanced Renewable Energy Systems*, 426–472. https://doi.org/10.1016/B978-1-78242-269-3.50017-6

Boehm, H. P. (2002). Surface oxides on carbon and their analysis: a critical assessment. *Carbon*, *40*(2), 145–149. https://doi.org/10.1016/S0008-6223(01)00165-8

Caballero, J. A., Font, R., & Marcilla, A. (1996). Comparative study of the pyrolysis of almond shells and their fractions, holocellulose and lignin. Product yields and kinetics. *Thermochimica Acta*, *276*(1–2), 57–77. https://doi.org/10.1016/0040-6031(95)02794-7

Cullis, C. F., & Hirschler, M. M. (1980). Atmospheric sulphur: Natural and man-made sources. *Atmospheric Environment (1967)*, *14*(11), 1263–1278. https://doi.org/10.1016/0004-6981(80)90228-0

Dumont, E., & Dumont, E. (2015). H2S removal from biogas using bioreactors: a review INTERNATIONAL JOURNAL OF ENERGY AND ENVIRONMENT H 2 S removal

from biogas using bioreactors: a review. In *International Journal of Energy and Environnement* (Vol. 6, Issue 5). Online. www.IJEE.IEEFoundation.org

Elsayed, Y., Seredych, M., Dallas, A., & Bandosz, T. J. (2009a). Desulfurization of air at high and low H2S concentrations. *Chemical Engineering Journal*, *155*(3), 594–602. https://doi.org/10.1016/J.CEJ.2009.08.010

Elsayed, Y., Seredych, M., Dallas, A., & Bandosz, T. J. (2009b). Desulfurization of air at high and low H2S concentrations. *Chemical Engineering Journal*, *155*(3), 594–602. https://doi.org/10.1016/J.CEJ.2009.08.010

González, J. F., Román, S., González-García, C. M., Nabais, J. M. V., & Ortiz, A. L. (2009). Porosity development in activated carbons prepared from walnut shells by carbon dioxide or steam activation. *Industrial and Engineering Chemistry Research*, *48*(16). https://doi.org/10.1021/ie801848x

Gordon G.E. (2000). Chapter 10 Sulfur compounds in the atmosphere. In *International Geophysics* (Vol. 71, Issue C). https://doi.org/10.1016/S0074-6142(00)80039-X

Guo, J., Luo, Y., Lua, A. C., Chi, R. an, Chen, Y. lin, Bao, X. ting, & Xiang, S. xin. (2007a). Adsorption of hydrogen sulphide (H2S) by activated carbons derived from oil-palm shell. *Carbon*, *45*(2), 330–336. https://doi.org/10.1016/J.CARBON.2006.09.016

Guo, J., Luo, Y., Lua, A. C., Chi, R. an, Chen, Y. lin, Bao, X. ting, & Xiang, S. xin. (2007b). Adsorption of hydrogen sulphide (H2S) by activated carbons derived from oil-palm shell. *Carbon*, *45*(2), 330–336. https://doi.org/10.1016/J.CARBON.2006.09.016

Gutiérrez Ortiz, F. J., Aguilera, P. G., & Ollero, P. (2014). Biogas desulfurization by adsorption on thermally treated sewage-sludge. *Separation and Purification Technology*, *123*, 200–213. https://doi.org/10.1016/J.SEPPUR.2013.12.025

Huang, C. C., Chen, C. H., & Chu, S. M. (2006). Effect of moisture on H2S adsorption by copper impregnated activated carbon. *Journal of Hazardous Materials*, *136*(3), 866–873. https://doi.org/10.1016/J.JHAZMAT.2006.01.025

Kambarova, G. B., & Sarymsakov, S. (2008). Preparation of activated charcoal from walnut shells. *Solid Fuel Chemistry*, *42*(3). https://doi.org/10.3103/S0361521908030129

Khabazipour, M., & Anbia, M. (2019). Removal of Hydrogen Sulfide from Gas Streams Using Porous Materials: A Review. In *Industrial and Engineering Chemistry Research* (Vol. 58, Issue 49, pp. 22133–22164). American Chemical Society. https://doi.org/10.1021/acs.iecr.9b03800

Luka, Y., Highina, B. K., & Zubairu, A. (2018). The Promising Precursors for Development of Activated Carbon: Agricultural Waste Materials- A Review. *International Journal of Advances in Scientific Research and Engineering*. https://doi.org/10.7324/ijasre.2018.32615

'Malone Rubright, S. L. ', 'Pearce, L. L. ', & 'Peterson, J. (2017). Environmental Toxicology of Hydrogen Sulfide. *US National Library of Medicine*.

McCabe W.L., Smith J.C., & Harriot P. (2005). *Unit operation of Chemical Engineering* (McGraw-Hill, Ed.; 7th ed.).

Meeyoo, V., Trimm, D. L., & Cant, N. W. (1997). Adsorption-Reaction Processes for the Removal of Hydrogen Sulphide from Gas Streams. *Journal of Chemical Technology & Biotechnology*, *68*(4). https://doi.org/10.1002/(sici)1097-4660(199704)68:4<411::aid-jctb644>3.3.co;2-0

Mohamad Nor, N., Lau, L. C., Lee, K. T., & Mohamed, A. R. (2013). Synthesis of activated carbon from lignocellulosic biomass and its applications in air pollution control—a review. *Journal of Environmental Chemical Engineering*, *1*(4), 658–666. https://doi.org/10.1016/J.JECE.2013.09.017

Nguyen-Thanh, D., & Bandosz, T. J. (2005). Activated carbons with metal containing bentonite binders as adsorbents of hydrogen sulfide. *Carbon*, *43*(2), 359–367. https://doi.org/10.1016/J.CARBON.2004.09.023

Nowicki, P., Skibiszewska, P., & Pietrzak, R. (2014). Hydrogen sulphide removal on carbonaceous adsorbents prepared from coffee industry waste materials. *Chemical Engineering Journal*, *248*, 208–215. https://doi.org/10.1016/J.CEJ.2014.03.052

Omri, A., Benzina, M., & Ammar, N. (2013). Preparation, modification and industrial application of activated carbon from almond shell. *Journal of Industrial and Engineering Chemistry*, *19*(6), 2092–2099. https://doi.org/10.1016/J.JIEC.2013.03.025

Panza, D. (2020). *Acido solfidrico: rischio chimico e sistemi di rimozione*.

Pipatmanomai, S., Kaewluan, S., & Vitidsant, T. (2009). Economic assessment of biogas-to-electricity generation system with H2S removal by activated carbon in small pig farm. *Applied Energy*, *86*(5), 669–674. https://doi.org/10.1016/J.APENERGY.2008.07.007

'Rigo, F., & 'Tronconi, L. (2020, December 22). *Emissioni in atmosfera: analidi del quadro legislativo*.

Rita D'orsogna, M., & Chou, T. (2010). *Danni alla salute umana causati dall'idrogeno solforato*.

Ryckebosch, E., Drouillon, M., & Vervaeren, H. (2011). Techniques for transformation of biogas to biomethane. In *Biomass and Bioenergy* (Vol. 35, Issue 5). https://doi.org/10.1016/j.biombioe.2011.02.033

Sing, K. S. W. (1985). Reporting physisorption data for gas/solid systems with special reference to the determination of surface area and porosity (Recommendations 1984). *Pure and Applied Chemistry*, *57*, 603–619.

Sitthikhankaew, R., Chadwick, D., Assabumrungrat, S., & Laosiripojana, N. (2014). Effects of humidity, O2, and CO2 on H2S adsorption onto upgraded and KOH impregnated activated carbons. *Fuel Processing Technology*, *124*, 249–257. https://doi.org/10.1016/J.FUPROC.2014.03.010

Speight, J. G. (2019). Unconventional gas. *Natural Gas*, 59–98. https://doi.org/10.1016/B978-0-12-809570-6.00003-5

Surra, E., Costa Nogueira, M., Bernardo, M., Lapa, N., Esteves, I., & Fonseca, I. (2019a). New adsorbents from maize cob wastes and anaerobic digestate for H2S removal from biogas. *Waste Management*, *94*, 136–145. https://doi.org/10.1016/J.WASMAN.2019.05.048

Surra, E., Costa Nogueira, M., Bernardo, M., Lapa, N., Esteves, I., & Fonseca, I. (2019b). New adsorbents from maize cob wastes and anaerobic digestate for H2S removal from biogas. *Waste Management*, *94*, 136–145. https://doi.org/10.1016/J.WASMAN.2019.05.048

van der Bruggen, B. (2014). Freundlich Isotherm. In *Encyclopedia of Membranes* (pp. 1–2). Springer Berlin Heidelberg. https://doi.org/10.1007/978-3-642-40872-4_254-3

WHO Regional Publication. (2000). *Air quality guidelines for Europe, 2nd Edition*.

Yang, L., & Ge, X. (2016). Chapter Three – Biogas and Syngas Upgrading. *Advances in Bioenergy*, *1*.

Resumen de Trabajo Fin de Máster
Ingeniería Química

Production of adsorbents derived from nut shells for H_2S removal

Autora: Angela Maiello

Tutor: Francisco Javier Gutiérrez Ortiz

Dpto. Ingeniería Química y Ambiental
Escuela Técnica Superior de Ingeniería
Universidad de Sevilla

Sevilla, 2022

La contaminación del aire se define como "cualquier cambio en la composición normal o el estado físico del aire atmosférico, debido a la presencia en el aire de una o más sustancias en cantidades y características tales que alteran las condiciones ambientales normales y saludables del aire; actividades y otros usos legítimos del medio ambiente; para alterar los recursos biológicos y los ecosistemas, así como los bienes públicos y privados", según la EPA. Como resultado, la contaminación del aire ocurre cuando cualquier sustancia, como gases, gotas y partículas, cambia la calidad del aire. En consecuencia, la contaminación del aire es un conjunto de consecuencias adversas que repercuten en la biosfera y, en consecuencia, en los seres humanos.

Es importante distinguir entre dos tipos de fuentes de contaminación:

- Natural, es decir, derivado de fuentes naturales.
- Antropogénico, es decir, causado por actividades humanas.

Las fuentes antropogénicas a su vez se dividen en:

- Fija, que puede ser pequeño o muy centralizado y de gran potencial.
- Móvil, por ejemplo, relacionado con el transporte.

Las fuentes antropogénicas tienen un impacto significativo en la calidad ambiental y están íntimamente ligadas a la generación y consumo de energía.

Debe investigarse el curso de tales interacciones, ya que pueden dar lugar al desarrollo de otros compuestos, que pueden ser más o menos peligrosos para los seres humanos y el medio ambiente. En este sentido, se puede distinguir entre:

- Contaminantes primarios, que son sustancias nocivas emitidas directamente a la atmósfera a partir del proceso que las produce, donde eventualmente sufren transformaciones fisicoquímicas.
- Contaminantes secundarios, que se producen por reacciones entre contaminantes primarios o entre contaminantes primarios y componentes atmosféricos naturales. Los contaminantes secundarios son el resultado de transformaciones fisicoquímicas, por ejemplo, por la acción de la radiación UV o la lluvia.

Los contaminantes están sujetos a fenómenos de difusión, dispersión y deposición luego de ser liberados a la atmósfera; además, pueden sufrir procesos de transformación químico-física que resulten en la producción de nuevos contaminantes.

Hasta el momento se han identificado aproximadamente 3000 contaminantes del aire, la mayoría de los cuales son creados por actividades humanas como procesos industriales, transporte u otros procesos antrópicos. Las formas de formación y liberación de los contaminantes son muy diversas, existiendo numerosos elementos que pueden afectar su difusión en la atmósfera.

Los principales contaminantes que se encuentran en la atmósfera son ciertamente el monóxido de carbono (CO), el dióxido de carbono (CO_2), los compuestos de nitrógeno (NOx), las partículas (PM) y entre estos también encontramos los compuestos de azufre (SOx).

Compuestos de azufre

El azufre es un elemento común que es vital para el ciclo del medio ambiente. Se encuentra principalmente como minerales de sulfuro y sulfato en la tierra, principalmente como sulfato disuelto en los océanos.

El dióxido de azufre, el azufre elemental, el ácido sulfúrico, el sulfuro de hidrógeno (junto con otras especies de azufre reducido) y los compuestos orgánicos de azufre son los compuestos de azufre más comunes que se encuentran en el medio ambiente.

Se ha reconocido la existencia de fuentes naturales de azufre en la atmósfera. Seguramente podemos ubicar las actividades geotérmicas entre las diferentes fuentes de emisión de compuestos de azufre a la atmósfera; sin embargo, los volcanes producen, con mucho, la mayor parte de las emisiones naturales de azufre; el dióxido de azufre es el compuesto de azufre más común liberado. A bajas temperaturas y en condiciones reductoras, el sulfuro de hidrógeno puede competir, y frecuentemente están presentes cantidades menores de trióxido de azufre, sulfato y azufre elemental.

El rocío fino, que se forma sobre los océanos y consiste en pequeñas gotas que se evaporan para dejar partículas sólidas aún más pequeñas, es otra fuente clave de azufre atmosférico.

La reducción biológica de los compuestos de azufre es una importante fuente natural de azufre en la atmósfera. Este tipo de reducción ocurre principalmente en presencia de materiales orgánicos y en ausencia de oxígeno. Los compuestos de azufre se liberan a la atmósfera a partir de la reducción de azufre no específica en algas marinas, suelos y plantas en descomposición, así como por bacterias que reducen selectivamente ciertos compuestos de azufre. Debido a la naturaleza cuantitativa de sus reacciones en la atmósfera, las cantidades de compuestos de azufre volátiles producidos por fuentes biogénicas son casi imposibles de detectar o calcular directamente.

Los compuestos de azufre no se acumulan en la atmósfera y, de hecho, existe un equilibrio entre el azufre que podemos encontrar en la atmósfera y su regreso a la superficie terrestre, pero los compuestos de sulfato hechos por el hombre y liberados a la atmósfera pueden cambiar drásticamente el punto de equilibrio.

El azufre total liberado a la atmósfera por los humanos, así como la influencia de sus actividades, ha ido en constante aumento a lo largo de los años. La combustión de carbón y petróleo, el refino del petróleo y la fundición de minerales no ferrosos son las principales fuentes industriales de azufre liberado a la atmósfera.

El carbón y sus derivados continúan siendo la fuente más abundante de azufre en la atmósfera. Debido al alto contenido de azufre del carbón, esta es una de las fuentes de emisiones más importantes. Las emisiones de azufre se pueden encontrar en la combustión industrial y de servicios públicos, así como en la combustión doméstica y de la industria a pequeña escala.

Los productos derivados del petróleo son otro importante productor de azufre en la atmósfera. En años anteriores, la fracción de azufre procedente del petróleo había alcanzado picos significativos. En este campo, el principal compuesto de azufre producido y emitido a la atmósfera es el dióxido de azufre.

Los compuestos de azufre también se liberan durante la fundición de minerales no ferrosos. El cobre es el mayor contribuyente, con el plomo y el zinc en segundo y tercer lugar, respectivamente. Este tipo de contaminación ha ido disminuyendo lentamente con el tiempo.

Se puede detectar un contenido significativo de azufre en muchos tipos diferentes de combustible: gas natural (GLP/biogás), diésel, aceites (ULSF, MGO/MDO, HFO (IFO)) y carbón. El azufre se encuentra en cantidades menores en el gas natural en comparación con otros combustibles, y se encuentra principalmente en forma de H_2S.

En los últimos años, las emisiones por el uso de combustibles que contiene azufre se han reducido considerablemente, gracias al uso de combustibles con un contenido de azufre mucho más bajo que antes. Además, gracias a las normas de emisión promulgadas entre 1990 y 2000, se ha detectado una reducción significativa de varios tipos de contaminantes, en particular los SOx (Ley de Aire Limpio). En un esfuerzo por proteger la calidad del aire en EE.UU, la Ley de Aire Limpio (CAA en inglés) se adoptó por primera vez en 1955 y luego se actualizó en 1990 y es la ley fundamental que rige la calidad del aire en los Estados Unidos de América. El propósito de la CAA es "proteger y mejorar la calidad de los recursos del aire de la Nación para promover la salud y el bienestar públicos y la capacidad productiva de su población". La Ley establece un marco regulatorio amplio y complicado para abordar las fuentes fijas y móviles de contaminación del aire. Requiere que se establezcan estándares mínimos nacionales de calidad del aire. Además, la Ley establece un sistema de permisos para todas las fuentes significativas de contaminación y aborda la prevención de la contaminación en áreas donde el aire está limpio.

Los compuestos de azufre son importantes en el medio ambiente y el sistema climático porque contribuyen a la generación de agotamiento del ozono, la producción de lluvia ácida y la corrosión de monumentos y metales.

Biogás

Los productos químicos peligrosos se vierten en la tierra, el aire y el agua como resultado de las actividades humanas, muchos de los cuales no son biodegradables y pueden causar daños duraderos. Los productos químicos que las actividades antropogénicas liberan a la atmósfera alteran la composición química del aire, provocando en ocasiones daños irreversibles en el medio ambiente y las estructuras, así como trastornos respiratorios, dermatológicos, inmunológicos, hepáticos, y diversos tipos de cáncer.

Para reducir la cantidad de CO_2 y otros contaminantes liberados a la atmósfera, es vital reducir el uso de combustibles fósiles y reemplazarlos por fuentes de energía renovables. Una de las fuentes de energía renovable más comunes, cuya producción está en constante crecimiento, es el biogás.

El biogás generalmente se refiere a un gas producido por la descomposición biológica de la materia orgánica en ausencia de oxígeno. El biogás es un tipo de biocombustible que está hecho de material biogénico, es decir, elementos biodegradables como biomasa, estiércol, aguas residuales, desechos urbanos, desechos verdes, material vegetal y cultivos energéticos que se digieren o fermentan anaeróbicamente.

El principal proceso de biodegradación que da lugar a la formación de biogás es la digestión anaerobia de sustancias orgánicas, realizada por un consorcio de microorganismos a través de una serie de etapas metabólicas (hidrólisis, acidogénesis, acetogénesis y metanogénesis), en las que diferentes cepas bacterianas se vuelven orgánicas complejas (líquidos o sólidos) en productos de bajo peso molecular. La degradación descontrolada de los residuos conduce también a la formación de biogás que, de no ser contenido oportunamente, puede dar lugar a importantes emisiones a la atmósfera. Por lo tanto, el término "biogás" abarca una amplia gama de gases resultantes de varios precursores, comenzando con varios desechos orgánicos como estiércol de ganado, desechos de alimentos y aguas residuales, que son fuentes potenciales de gas biogénico o biogás, que generalmente se considera una fuente de energía renovable y, a menudo, se clasifica según la fuente.

Desde el punto de vista de la composición, el biogás es una fuente de energía sostenible que consiste principalmente en metano (CH_4) y dióxido de carbono (CO_2). Varios gases menores incluyen nitrógeno (N2), vapor de agua (H2O), amoníaco (NH3), sulfuro de hidrógeno (H_2S) y otros compuestos de azufre. El biogás también puede contener siloxanos, hidrocarburos halogenados y compuestos orgánicos volátiles (COV), dependiendo del sitio de producción (vertederos, plantas de tratamiento de aguas residuales, plantas que manejan desechos industriales o de alimentos).

El biogás tiene un alto poder calorífico debido a su alta concentración de metano, por lo que puede ser utilizado como combustible renovable. El biogás también se puede utilizar como combustible de bajo costo, por lo que se puede usar para generar electricidad, calor y, al igual que el gas natural, se puede comprimir para usarlo como biocombustible para vehículos de motor.

El biogás debe limpiarse (principalmente eliminando H_2O, H_2S y siloxanos) y posiblemente mejorarse (eliminación de CO_2) antes de que pueda utilizarse como fuente de energía (biometano) para generar calor y energía.

Los niveles de H_2S en el biogás normalmente varían de 50 a 5000 ppmv, pero en ciertas situaciones pueden superar las 20 000 ppmv (2% en volumen). Los principales problemas causados por las altas concentraciones de H_2S en el biogás son (i) su actividad corrosiva, que puede dañar motores, tuberías, compresores, tanques de almacenamiento de gas y (ii) la formación de óxidos de azufre (SOx) como resultado de la combustión de H_2S. En consecuencia, se debe disminuir el contenido de H_2S en el biogás a valores que no perjudiquen los procesos de combustión ni provoquen emisiones de SOx.

Contaminantes del biogás: Sulfuro de hidrógeno (H_2S)

Entre las sustancias no deseadas comúnmente presentes en el biogás, el compuesto de interés para el presente trabajo es el sulfuro de hidrógeno (H_2S).

El sulfuro de hidrógeno es un gas incoloro con el olor fétido característico de los huevos podridos, por lo que se le llama gas pútrido. No tiene cualidades ácidas en su estado anhidro, pero se manifiesta en presencia de H2O, cuando forma sulfuros y sulhidratos acuosos.

La percepción olfativa de este químico es notablemente baja. Es un gas venenoso y altamente combustible que puede surgir cuando se expone al aire en cantidades específicas. Puede tener tanto orígenes naturales, ya que está presente en las emisiones de zonas geotérmicas y volcánicas y se produce por la degradación bacteriana de proteínas animales y vegetales, como antropogénicos.

El origen antrópogénico se remonta a procesos como la fabricación de carbón coquizable, el refino de petróleo, la fabricación de fertilizantes, el tratamiento de aguas residuales y otros procesos industriales en los que es un subproducto no deseado. El sulfuro de hidrógeno es el principal subproducto de la hidrodesulfuración del petróleo y se puede encontrar como componente inherente del petróleo natural o como subproducto de la síntesis de una sustancia.

El sulfuro de hidrógeno es sumamente venenoso y desagradable, además de asfixiante. Paraliza el nervio olfativo a altas concentraciones, haciendo imposible detectar su mal olor. Los ojos y la garganta se irritan por la exposición de bajo nivel. Puede causar cansancio, pérdida de apetito, dolores de cabeza, problemas de memoria y desorientación a largo plazo. Las concentraciones superiores a 1000 ppm provocan un colapso instantáneo por asfixia, incluso después de una sola respiración, y el límite de exposición libre de daños para un día de 8 horas es inferior a 10 ppm.

El gas es inflamable y, a temperaturas superiores a 260 °C, arde con una llama azulada. Las concentraciones de H_2S en el aire superiores al 4% son explosivas. Debido a que los radicales hidroxilo y otros oxidantes atmosféricos oxidan rápidamente el H2S a SO2 y luego a sulfato, el tiempo de residencia del H_2S emitido en la atmósfera es corto (alrededor de 15 días).

Como resultado, las concentraciones de H_2S en las regiones rurales oscilan entre 0,02 y 0,3 ppb. Las concentraciones de H_2S pueden superar fácilmente el nivel de umbral olfativo de 0,02 ppm en lugares con actividad volcánica y producción industrial o animal contaminante. Además, las concentraciones de H_2S en el aire cerca de volcanes y pozos geotérmicos pueden acercarse a 0,1 ppm. La mitad de la población puede detectar el olor acre del H_2S en cantidades tan bajas como 8 ppb, y el 90 % puede detectar su olor habitual en 50 ppb.

Las formas en que el sulfuro de hidrógeno ingresa al cuerpo humano son tres:

- por inhalación a través de los pulmones.
- por vía oral, especialmente por la digestión de sustancias contaminadas absorbidas en el tracto intestinal, en primer lugar, el agua.
- a través de la piel.

Regulación de emisiones

Las emisiones a la atmósfera se abordan a nivel europeo de diversas maneras; en particular, se pueden distinguir la legislación sobre emisiones industriales y la regulación sobre calidad del aire ambiente. La Directiva 2010/75/CE regula las emisiones de los establecimientos industriales. Las referencias clave para los estándares de calidad del aire ambiental son las siguientes:

• La Directiva 2004/107/CE se refiere al arsénico, cadmio, mercurio, níquel e hidrocarburos aromáticos en el aire ambiente.

• Directiva 2008/50/CE, que consolida en un único texto legislativo algunas directivas existentes sobre calidad del aire y límites de emisión.

• Directiva 2016/2284/UE, por la que se modifica la Directiva 2003/35/CE y se deroga la Directiva 2001/81/CE y se trata de la reducción de las emisiones nacionales de determinados contaminantes atmosféricos.

La Directiva 2016/2282/UE establece nuevos compromisos nacionales para reducir las emisiones antropógenas de dióxido de azufre, óxido de nitrógeno, amoníaco, compuestos orgánicos volátiles y partículas finas. Con este fin, los Estados miembros de la UE están obligados a adoptar e implementar programas nacionales de control de la contaminación; además, se planean medidas para monitorear los contaminantes y los impactos adversos de la contaminación del aire en los ecosistemas, así como los requisitos de notificación de los datos recopilados.

El objetivo es alcanzar los objetivos de calidad del aire a largo plazo propugnados tanto por la Organización Mundial de la Salud (OMS) como por la Unión Europea en las áreas de biodiversidad, protección de ecosistemas, clima y energía.

Los valores límite, los umbrales de alarma y/o los valores objetivo de calidad del aire para el sulfuro de hidrógeno no están definidos en la legislación europea. En ausencia de referencias normativas, es una práctica común a nivel nacional e internacional recurrir a los valores guía de la OMS.

Técnicas de eliminación de H_2S

Dado que la eliminación de H_2S es necesaria para evitar daños en los equipos y problemas de envenenamiento ambiental relacionados con la emisión de compuestos de azufre, se han adoptado varias técnicas para eliminar el sulfuro de hidrógeno de la corriente de biogás, como absorción física/química, precipitación de cloruro de hierro , adsorción de óxidos/hidróxidos metálicos, permeación de membranas, métodos biológicos y adsorción sobre carbón activado; este último es de especial interés para nosotros.

Deben identificarse, planificarse, implementarse y administrarse adecuadamente los sistemas apropiados de recolección y eliminación de gases para evitar los peligros asociados con la exposición al sulfuro de hidrógeno.

En general, los métodos de eliminación de H_2S se pueden dividir en dos categorías según sus principios: métodos físicos-químicos tradicionales y métodos biológicos. Las soluciones biológicas han avanzado significativamente en los últimos años, debido a su alta eficiencia de remoción (> 99%) y costes operativos más económicos en comparación con los procedimientos fisicoquímicos. También se han desarrollado métodos que combinan tecnologías fisicoquímicas y biológicas.

La eliminación de H_2S se puede realizar in situ, es decir, directamente en el digestor, o después de la digestión, ex situ. Los métodos in situ más utilizados son:

- Adición de sales/óxidos de hierro en el digestor.
- Dosificación de aire/oxígeno en el digestor.

Los cloruros, fosfatos u óxidos de hierro se pueden agregar directamente al digestor o al sustrato de alimentación del tanque de almacenamiento previo. El método más utilizado es añadir $FeCl_2$. También se pueden utilizar cloruro ferroso ($FeCl_3$) e hidróxido de hierro ($Fe(OH)_3$ o $Fe(OH)_2$) en forma sólida. Luego, reaccionan con sulfuro de hidrógeno para producir sales de sulfuro de hierro insolubles (FeS).

Este enfoque es muy eficiente para reducir los niveles altos de H_2S, pero es menos efectivo para lograr un nivel de H_2S bajo y estable en el rango de demandas de inyección de vehículos y redes de gas. En promedio, permite reducir las concentraciones de H_2S en el biogás a un valor entre 200 y 100 ppm. Se requiere un exceso considerable de iones de hierro para la eliminación a concentraciones más bajas. Este método solo puede considerarse un proceso de eliminación parcial en este momento y debe usarse junto con otra tecnología para lograr una reducción de 10 ppmv.

La adición de aire u oxígeno directamente al digestor o al tanque de almacenamiento es otro método in situ. Esta técnica se basa en la oxidación aeróbica biológica de H_2S a azufre elemental o sulfatos realizada por la bacteria Thiobacillus. La mayoría de esas bacterias oxidantes de sulfuro son autótrofas, por lo que utilizan carbono inorgánico como fuente de carbono (CO_2 del biogás). No requieren

inoculación y crecen en la superficie del digestato o en la estructura del digestor.

Una pequeña cantidad de O_2 (2-6%), necesaria para que se produzca la reacción, se introduce en el biogás, por ejemplo, utilizando una bomba de aire. Se pueden lograr reducciones de H_2S del 80 al 99 %, hasta 20 a 200 ppm, según la temperatura, el tiempo de respuesta y el volumen y la ubicación del aire. Sin embargo, la concentración restante puede ser demasiado alta para que el biogás se utilice como alternativa al gas natural.

Las técnicas de eliminación de sulfuro de hidrógeno (ex-situ) se clasifican de la siguiente manera:

- Biológicos (p. ej., biofiltros, biodepuradores, lodos activados).
- Físico - Químico (p. ej., adsorción con carbón activado, absorción con agua, absorción química, depuradores químicos, purificación por membrana).

En los biofiltros, el sulfuro de hidrógeno es degradado biológicamente por microorganismos que colonizan un medio orgánico y convierten el sulfuro de hidrógeno en azufre elemental y ácido sulfúrico, a partir de los cuales se forman los sulfatos. Debido a que los microorganismos empleados para eliminar el H_2S son aeróbicos, requieren oxígeno. El método tradicional de proporcionar oxígeno a un biofiltro es inyectar aire (4-10 %) directamente en la corriente de gas. Los biodepuradores y los filtros biotrucadores, que utilizan un medio inorgánico, son una alternativa a los biofiltros. Los biofiltros y los biofiltros percoladores se diferencian principalmente en el tipo de material portador, que es orgánico en los biofiltros e inerte en los biofiltros percoladores. Como los nutrientes no están presentes en el material del filtro biopercolador, estos se proporcionan a los microorganismos recirculando una fase líquida a través del reactor de forma continua. Los biodepuradores están compuestos por dos reactores de columna: en el primero, el material es absorbido por el líquido a contracorriente en un lecho empacado; en el segundo, donde se descarga el líquido del primer reactor, los procesos degradativos son desarrollados por bacterias específicas. La ausencia de inyección de oxígeno o nitrógeno en la corriente de biogás es una ventaja de este procedimiento en comparación con los biofiltros/filtros biopercoladores. Los costes operativos específicos más altos son las desventajas asociadas.

En la absorción física, el H_2S se elimina por absorción en agua u otros disolventes, como el metanol. La absorción química, por su parte, se produce en torres de lavado o lavadores, normalmente en lecho empacado, donde el gas a tratar entra en contacto con la solución líquida absorbente en un flujo a contracorriente, pasando el gas a través de la fase líquida. Se pueden utilizar diferentes tipos de soluciones para eliminar el sulfuro de hidrógeno (por ejemplo, hidróxido de sodio, peróxido de hidrógeno, etc.). El principal inconveniente de la absorción es que, por lo general, resuelve un problema con una corriente de gas contaminada al crear una corriente de líquido contaminado que debe tratarse más. Otros inconvenientes incluyen un alto costo de inversión inicial, así como un uso significativo de agua y/o productos químicos. La alta eficiencia de eliminación (hasta el 99 %), el tamaño reducido y la capacidad de gestionar una amplia variedad de concentraciones de contaminantes son todas ventajas.

La separación por membranan implica el uso de membranas semipermeables para separar el H_2S de una corriente de gas mediante la creación de un gradiente de presión parcial a lo largo de la superficie vítrea o gomosa semipermeable de la membrana. La membrana está diseñada para permitir el paso preferencial de gases o moléculas contaminantes a través de ella, lo que resulta en una corriente contaminante más concentrada en un lado. Existen dos tipos de sistemas de membrana: alta presión con fase gaseosa en ambos lados y baja presión con un adsorbente líquido en un lado. Debido a su alto costo, la separación por membrana aún no es competitiva para la eliminación selectiva de H_2S.

Por último, la adsorción es el proceso químico-físico mediante el cual se captura un gas en la superficie de un material sólido, como el carbón activado o material cristalino con alta porosidad interna (por ejemplo, gel de sílice, zeolitas). Una vez capturado el contaminante y saturado el sólido, los materiales de adsorción deben regenerarse o desecharse. En general, la adsorción con carbón activado se emplea para concentraciones bajas de contaminantes; para niveles mayores se debe utilizar carbón impregnado o carbón catalítico. La adsorción es una de las más competitivas.

Con el fin de maximizar la eficiencia de remoción, los métodos antes mencionados se emplean frecuentemente en conjunto, dependiendo de la calidad y características del gas a tratar y el grado de sulfuro de hidrógeno presente.

Objetivo del estudio

En esta investigación, se empleó la adsorción para eliminar el H_2S del biogás simulado. La adsorción es un proceso eficiente para la eliminación de H_2S y el carbón activado se emplea comúnmente como adsorbente.

Dado el alto costo de eliminar el sulfuro de hidrógeno de las corrientes gaseosas mediante adsorción con carbón activado comercial, existe una gran atención e interés en desarrollar nuevos adsorbentes a partir de precursores naturales, como los desechos orgánicos, para generar adsorbentes de bajo costo. En esta investigación se utilizaron cáscaras de nueces y almendras, que se descubrió que eran desechos del sector alimentario. Para ello se ensayaron diferentes tratamientos térmicos para la activación de estos precursores y para generar diferentes adsorbentes.

El principal objetivo de esta investigación es evaluar la capacidad de adsorción de H_2S de los adsorbentes producidos, individualizando simultáneamente los de mejor rendimiento entre los sintetizados.

Esto nos permite determinar cuáles de los adsorbentes creados pueden emplearse como sustituto o complemento de los carbones activados comerciales para eliminar el sulfuro de hidrógeno de las corrientes gaseosas, particularmente del biogás.

El estudio experimental se llevó a cabo en el Departamento de Ingeniería Química y Ambiental de la Universidad de Sevilla.

Para producir adsorbentes, inicialmente se utilizaron un molino de mandíbulas y un molino de cuchillas para moler las conchas; luego se utilizó un tamiz electromagnético para obtener el tamaño de grano deseado; y finalmente, se utilizó un horno tubular para los pasos de activación, lo que condujo a la producción de los adsorbentes finales. Para las campañas experimentales de adsorción se empleó una columna de lecho fijo, con una altura de 430 mm y un diámetro de 30 mm. Se realizaron pruebas experimentales a temperatura ambiente y presión atmosférica, con el objetivo de probar la capacidad de adsorción de H_2S de los adsorbentes producidos, seleccionando el mejor rendimiento para la desulfuración de un biogás modelo.